Tectonics

RESEARCH ARTICLE
10.1029/2019TC005524

Special Section:
Tectonic evolution of West-Central Tethysides

Coupled Crust-Mantle Response to Slab Tearing, Bending, and Rollback Along the Dinaride-Hellenide Orogen

Mark R. Handy[1], Joerg Giese[1,2], Stefan M. Schmid[3], Jan Pleuger[1], Wim Spakman[4,5], Kujtim Onuzi[6], and Kamil Ustaszewski[7]

[1]Freie Universität Berlin, Berlin, Germany, [2]Geological Survey of Norway, Trondheim, Norway, [3]ETH Zürich, Zürich, Switzerland, [4]Institute of Earth Sciences, Utrecht University, Utrecht, the Netherlands, [5]Centre of Earth Evolution and Dynamics (CEED), University of Oslo, Oslo, Norway, [6]Instituti i Gjeoshkencave, Energjise, Ujit dhe Mjedisit, Tirane, Albania, [7]Friedrich-Schiller-Universität Jena, Jena, Germany

Abstract We integrate structural, geophysical, and geodetic studies showing that the Dinarides-Hellenides orogen along the Adria-Europe plate boundary in the Western Balkan peninsula has experienced clockwise oroclinal bending since Eocene-Oligocene time. Rotation of the Hellenic segment of this orogen has accelerated since the middle Miocene and is associated with a north-to-south increase in shortening along the orogenic front. Within the Paleogene nappe pile, bending was accommodated by orogen-parallel extension, clockwise block rotation, and thrusting in the hanging wall of the Skhoder-Peja Normal Fault (SPNF). The SPNF and related faults cut the older Skhoder-Peja Transfer Zone with its pre-Neogene dextral offset of the West Vardar ophiolite nappe. Rotation of the SPNF hanging wall involved Miocene-to-recent, out-of-sequence thrusting that was transferred to the Hellenic orogenic front via lateral ramps on dextral transfer zones. Along strike of the Dinarides-Hellenides and coincident with the southward increase in Neogene shortening, the depth of the Adriatic slab increases from ~160 km north of the SPNF to ~200 km just to the south thereof, to several hundreds of kilometers to the south of the Kefalonia Transfer Zone. The geodynamic driver of tectonics since the early Miocene has been enhanced rollback of the Hellenic segment of the Adriatic slab in the aftermath of Eocene-Oligocene slab tearing and breakoff beneath the Dinarides, which focused slab pull in the south. The SW-retreating Hellenic slab segment induced clockwise bending of the southern Dinarides and northern Hellenides, including their Adriatic foreland, about a rotation pole in the vicinity of the Mid-Adriatic Ridge.

Key Points:
- The junction of the Dinarides and Hellenides is the site of a N-to-S increase in Neogene shortening and upper-plate extension
- This shortening reflects oroclinal bending about a pole near the Mid-Adriatic Ridge that has been driven by Hellenic rollback subduction
- The Shkoder-Peja Normal Fault accommodated Neogene orogen-parallel extension and clockwise rotation of shallower levels of the orogen

Supporting Information:
- Supporting Information S1
- Movie S1
- Movie S2

Correspondence to:
M. R. Handy,
mark.handy@fu-berlin.de

Citation:
Handy, M. R., Giese, J., Schmid, S. M., Pleuger, J., Spakman, W., Onuzi, K., & Ustaszewski, K. (2019). Coupled crust-mantle response to slab tearing, bending, and rollback along the Dinaride-Hellenide orogen. *Tectonics*, *38*, 2803–2828. https://doi.org/10.1029/2019TC005524

Received 18 FEB 2019
Accepted 30 MAY 2019
Accepted article online 17 JUN 2019
Published online 7 AUG 2019

1. Introduction

Convergence of the African and European plates in the Mediterranean area is accommodated by microplates such as the Adriatic Plate with arcuate, often diffuse boundaries along which subduction mechanisms and convergence rates vary (Faccenna et al., 2003). The question arises of how the crust accommodates such along-strike differences, specifically, of how extension and block rotation are related to thrusting in orogens such as the Dinarides-Hellenides forming the upper plate above the subducting Adriatic microplate (Figure 1).

The Dinarides-Hellenides orogen is a SW-vergent fold-and-thrust belt that initiated during Late Jurassic to Early Cretaceous obduction of Neotethyan Vardar ophiolites (Bortolotti et al., 2013; Gawlick et al., 2008, 2016; Tremblay et al., 2015) and grew during subsequent collision of the Adriatic and European Plates (Schmid et al., 2008; Ustaszewski et al., 2010). West Vardar ophiolites are those Vardar ophiolites (undifferentiated in Figure 2) located west of the Sava Suture Zone. This suture is the Adria-Europe boundary (Pamić, 2002; Figure 1) where the last part of the Neotethyan Ocean was subducted (Gallhofer et al., 2015; Prelević et al., 2017; Schmid et al., 2008). Suturing occurred no later than 65 Ma, when siliciclastic foredeep sediments in this suture zone reached amphibolite-facies peak metamorphic conditions (Ustaszewski et al., 2010, and references therein).

The Dinaric and Hellenic segments of this orogen are separated by two prominent structures: (1) the NE-SW trending Shkoder-Peja Transverse Zone (SPTZ), a zone of dextral offset between the cities of Shkoder and Peja (Figure 2), and (2) a corridor of orogen-parallel extension, the most prominent structure of which is a normal fault, the Shkoder-Peja Normal Fault (SPNF), that cuts the fold-and-thrust belt and overprints structures of the SPTZ. The SPTZ coincides with orogen-parallel changes in the facies of

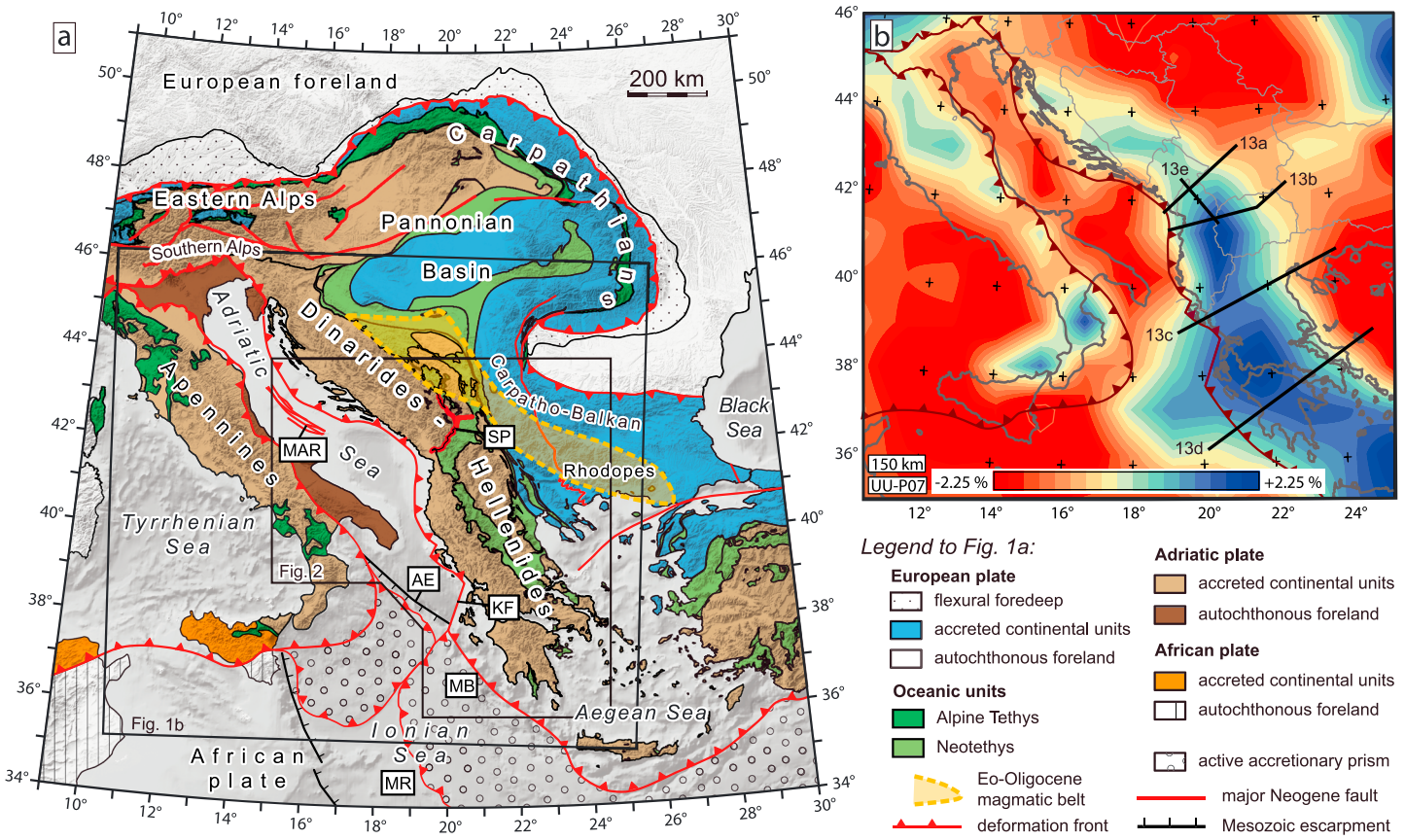

Figure 1. Africa-Europe convergence zone with (a) Alpine chains of the central Mediterranean and their accreted European (blue) and Adriatic crust (brown). Box shows location of teleseismic *P* wave anomaly map at 150-km depth in (b). Belt of Eocene-Oligocene magmatism (orange) discussed in text and compiled from Harangi et al. (2006), their Figure 5), Péskay et al. (2006), their Figure 4), Seghedi and Downes (2011), their Figure 3) in the Carpathian–Pannonian area, and Schefer et al. (2011) in the Dinarides. Black lines in (b) mark locations of cross sections in Figure 14. *P* wave tomography based on model UU-P07 of Hall and Spakman (2015). AE = Adriatic Escarpment; KF = Kefalonia Transform; MAR = Mid-Adriatic Ridge; MB = Mediterranean Backstop; MR = Mediterranean Ridge; SP = Shkoder-Peja Normal Fault.

Mesozoic strata, which Aubouin and Dercourt (1975) interpreted as the expression of an even older, NE-SW trending, Mesozoic transverse zone (their "Transversale de Scutari-Pec," not shown in the figures). The SPTZ and SPNF also coincide with an 80-km, right-lateral offset of the ophiolite front, as well as with a clockwise oroclinal bend of ~30°, from a NW-SE Dinaric trend north of the SPNF to a NNW-SSE Hellenic trend south thereof (Figure 1b). However, the Sava Suture Zone is not offset by the SPTZ and SPNF (Figure 2).

The segment of the orogen in Albania is sometimes referred to as the Albanides (Cvijić, 1901; Meço & Aliaj, 2000). However, the nappe structure of this segment is identical with the northwestern Hellenides (e.g., Schmid et al., 2011, map downloadable from https://tecto.earth.unibas.ch//images/ALCADI_2016_01_30.png), so that we opt for the more widely used term "Hellenides" in this paper.

We note that the names of the Dinaric and Hellenic nappes used in this paper are often the same as those given to Mesozoic facies zones in the Adriatic region. The latter trend NW-SE (Bernoulli, 2001), oblique to subparallel to the strike of the Dinarides-Hellenides nappes. The nappes are distinguished from the facies zones by the age and provenance of flysch forming the stratigraphically highest members of each nappe. The flysch ages in the nappe pile decrease from Late Cretaceous in the NE to Miocene in the SW (Xhomo et al., 1999), reflecting southwestward propagation of the Dinaric-Hellenic foredeep and nappe stacking (e.g., Pamić et al., 1998; Robertson & Shallo, 2000; Schmid et al., 2008; van Hinsbergen et al., 2005).

Regarded on the plate scale, the Dinarides-Hellenides junction marks a strike-parallel change in Tertiary kinematics, from oblique dextral convergence with negligible post-late Oligocene rotation of the Dinarides

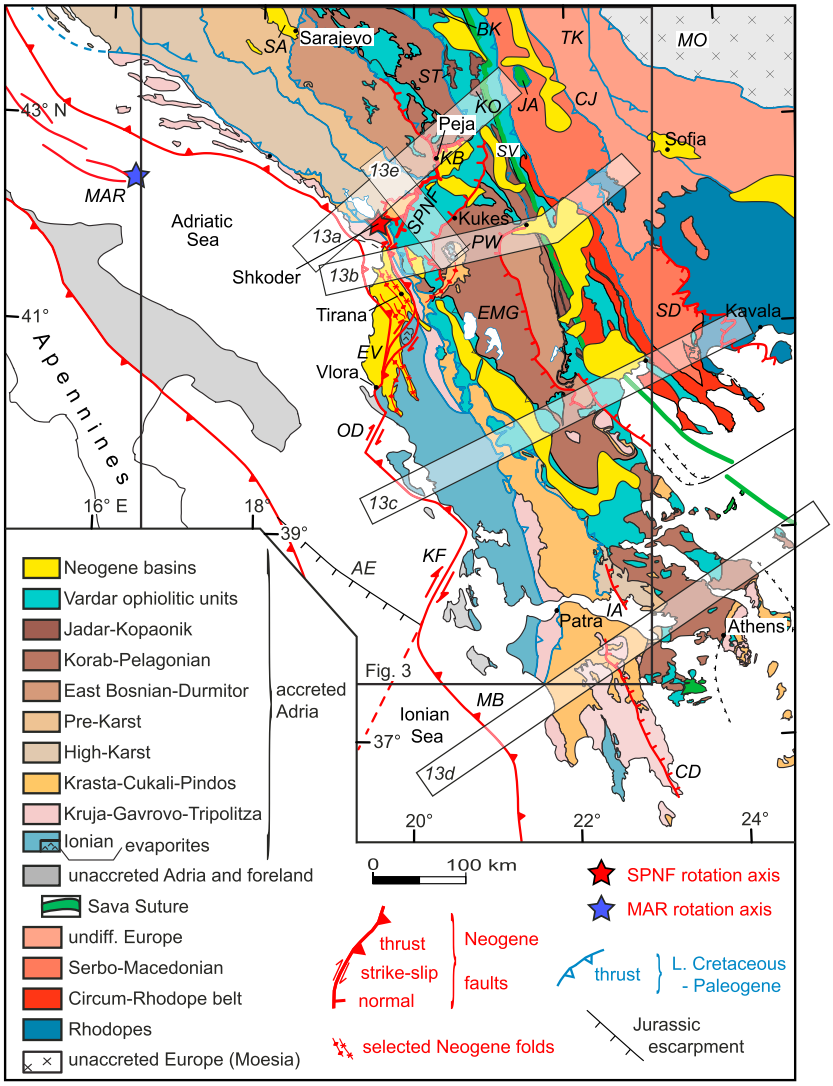

Figure 2. Tectonic map of the Dinarides-Hellenides orogen including the SPNF and other Neogene faults in red; red star represents vertical clockwise rotation axis of the SPNF hanging wall. Blue star represents proposed clockwise rotation axis for southern Dinarides and northern Hellenides (see text), and green line represents Sava Suture Zone. Map modified from Schmid et al. (2008, 2011). AE = Adriatic Escarpment; BK = Bukulja core complex; CD = Cretan Detachment; CJ = Cerna-Jiu; EMG = East Mainland Greece Detachment; EV = Elbasan-Vlora Transfer Zone; IA = Itea-Amphissa Detachment; JA = Jastrebac core complex; KB = Kosovo-Metohia Basin; KF = Kefalonia Transfer Zone; KO = Kopaonik core complex; MAR = Mid-Adriatic Ridge; MB = Mediterranean Backstop; MO = Moesia; OD = Othoni-Dhermi Transfer Fault; PW = Peshkopie Window; SA = Sarajevo Basin; SD = Strimon Valley Detachment; SPNF = Shkoder-Peja Normal Fault; ST = Studenica core complex; SV = Sava Suture Zone; TK = Timok Fault; Locations of CD, EG, IA, and SD from Brun and Soukoutis (2010), van Hinsbergen and Schmid (2012), and Georgiev et al. (2010).

with respect to Europe (de Leeuw et al., 2012, and references cited therein) to SW-retreating subduction and Mio-Pliocene clockwise rotation of the northern Hellenides with respect to both Europe and Africa (Kissel et al., 1995; Speranza et al., 1995). Therefore, several authors have placed the pole of clockwise rotation of the northern Hellenides along the SPTZ (e.g., Brun & Soukoutis, 2010; Kissel et al., 1995; Walcott & White, 1998). In contrast, the Adriatic plate has rotated counterclockwise with respect to Europe (e.g., Marton et al., 2003), with recent estimates of rotation over the past 20 Ma ranging from 20° (Ustaszewski et al., 2008) to 5° (Le Breton et al., 2017) or even less (see discussion in van Hinsbergen et al., 2014). Counterclockwise rotation of Adria with respect to Europe agrees with geodetic studies showing a current NW-to-SE, orogen-parallel increase in Adria-Europe convergence rate from 2 to 4 mm/year (D'Agostino et al., 2008; Vrabec et al., 2006). Seismic-moment and geodetic workers place the vertical pole of this

rotation at the NW corner of the Adriatic microplate, within the arc of the Western Alps (Anderson & Jackson, 1987; Nocquet & Calais, 2004; Vrabec et al., 2006; Bennett et al., 2012, and references therein). All of these studies assume that Adria moved as a single microplate, though other investigations suggest that it fragmented into two blocks or subplates which are currently rotating in opposite senses, with respect to each other, as well as relative to Europe and Africa (D'Agostino et al., 2008; Sani et al., 2016; Scisciani & Calamita, 2009). We will refer to these northern and southern subplates, respectively, as Adria sensu stricto (s.str.) and Apulia (D'Agostino et al., 2008; Oldow et al., 2002) to avoid confusion with the widespread term Adriatic Plate or Adria (Channell et al., 1979) which includes both subplates. The Dinarides-Hellenides junction is therefore an obvious place to search for traces of differential motion between the subplates of Adria, the northern Hellenides, Africa and Europe.

Teleseismic tomography reveals a positive NE-dipping velocity anomaly beneath the Dinarides, interpreted as a slab of subducted and partly torn Adriatic lithosphere (Figure 1b, Bijwaard & Spakman, 2000; Wortel & Spakman, 2000; Piromallo & Morelli, 2003). The slab becomes progressively longer when going to the southeast along strike of northwestern Hellenides (e.g., Piromallo & Morelli, 2003; Spakman & Wortel, 2004). In light of significant late Paleogene-Neogene upper-plate extension in the Aegean (e.g., Brun et al., 2016) and SE-Balkans (e.g., Burchfiel et al., 2008), this increase in slab length has been attributed to an increase in the amount of rollback subduction going along strike from the Dinarides-Hellenides junction to the apex of the Hellenic orogenic arc (e.g., Jolivet & Brun, 2010). Linking rollback of the descending Adriatic plate to rotation and extension of the upper plate yields fresh insight into how motion of the mantle lithosphere is transferred through the crust to the surface during subduction.

In this paper, we synthesize new and existing geological and geophysical data to shed light on the way that orogenic lithosphere responds to lateral variations in the modes of subduction and collision. We show that the SPNF and related normal faults at the Dinarides-Hellenides junction accommodated orogen-parallel and orogen-normal extension combined with clockwise rotation of a large crustal block in the hanging wall of the SPNF. This rotational extension is linked to out-of-sequence thrusting and dextral transfer faulting along the orogenic front of the northwestern Hellenides. We then review structural, paleomagnetic, and seismological evidence that this block rotation and transfer faulting partly accommodated clockwise bending of the entire Dinarides-Hellenides orogen and the down-going slab. Finally, we relate this oroclinal bending to changes in the amount of retreat of the Adria-Europe plate interface as quantified in new cross sections constructed across the southern Dinarides and northwestern Hellenides. This highlights the role of slab rollback in deforming and fragmenting the Adriatic plate, as well as reveals the mechanisms of coupling between the upper and lower plates during retreat and arcuation of the Hellenic subduction zone.

2. Neogene Orogen-Parallel and Orogen-Normal Extension

Already at the beginning of the last century, geological mapping at the junction of the Dinarides and Hellenides revealed a structural dome (the Cukali Dome) flanked by faults that trend oblique to the orogen (Cvijić, 1901) and cut nappe contacts and SW-vergent postnappe folds (Nopcsa, 1911). Our own detailed mapping reveals that these faults are part of a system of brittle normal faults that delimit a NE-SW trending graben. This graben contains the nappe stack topped by obducted Neotethyan ophiolite (West Vardar Ophiolite Zone; sensu Schmid et al., 2008) discordantly overlain by lower Cretaceous limestone (Xhomo et al., 1999) and Mio-Pliocene fill (latter shown in Figure 3). At the surface, the SPNF delimiting this graben structure in the NW dips 30–40° to the SE, truncating SW-vergent Dinaric folds exposed in the Cukali Dome in its footwall (Nopcsa, 1911). North of Peja, the SPNF bifurcates; one branch runs to the NW, reactivating a thrust between internal Dinaric nappes (Figure 3), whereas the other branch bounds the mid-Miocene to Pliocene Kosovo-Metohia Basin (e.g., Elezaj, 2009; Figure 3a). In existing cross sections of this basin (Legler et al., 2006; Elezaj, 2009, his Figure 4), Miocene clastic strata thicken to the WSW, that is, toward the SPNF. This indicates that they were deposited in the hanging wall of the SPNF and places a younger age limit on normal faulting.

In detail, the SPNF near Bajram Curri in northern Albania (Figure 4a) features sheared bedding in its footwall and cataclasites containing fault planes (Figures 4b and 4c) with striae indicating top-S to top-SE hanging wall motion (Figure 3). The deepest unit offset by this fault is the Krasta-Cukali nappe with a

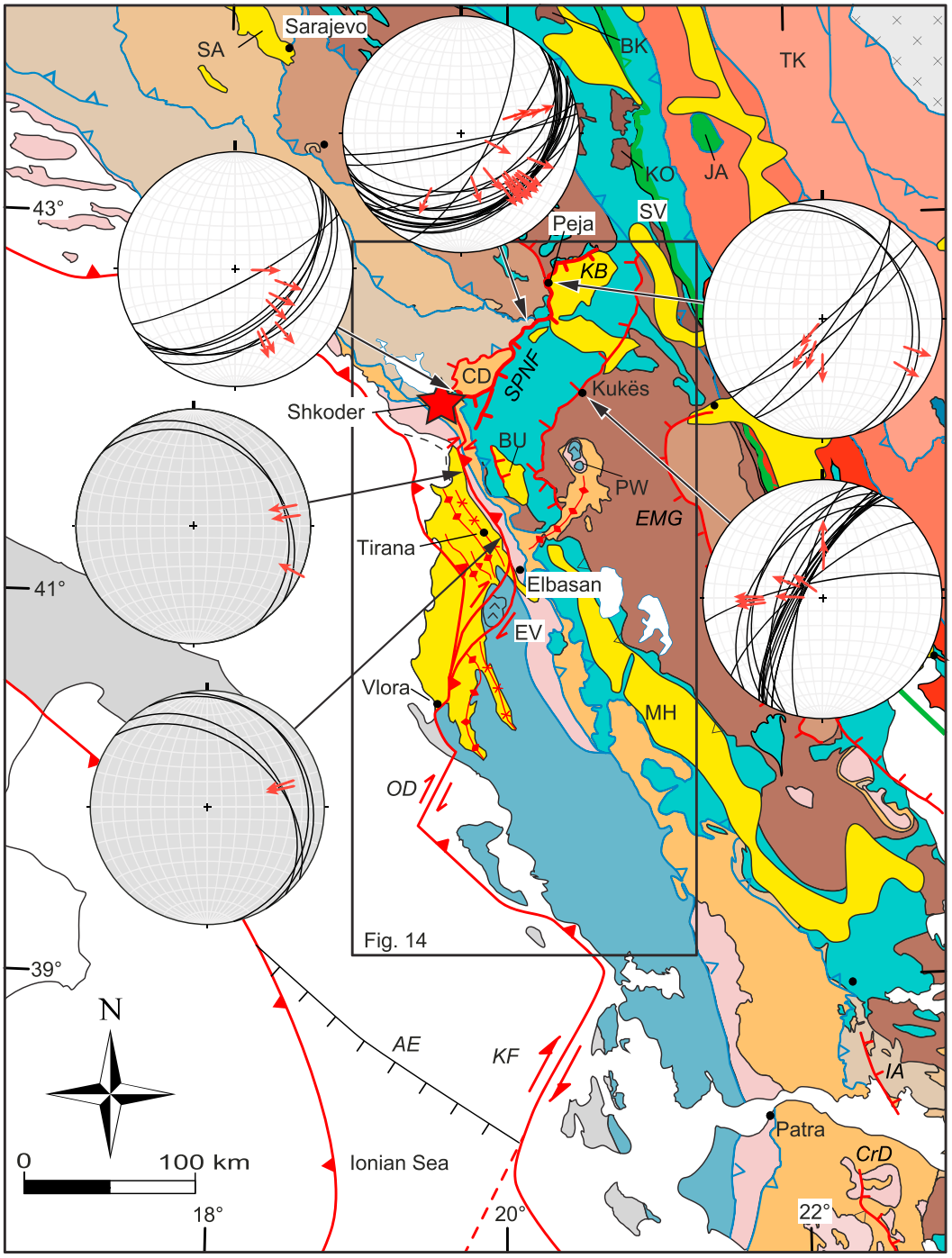

Figure 3. SPNF and coeval thrusts and transfer zones marked in red. Neogene basins coloured yellow. Lower hemisphere equal-area plots of fault planes (great circles, black) and hanging wall motion (red arrows) for thrusts (gray plots) and normal faults (white plots). Symbols and tectonics units as in Figure 1. AE = Adriatic Escarpment; BK = Bukulja core complex; BU = Burell Basin; CD = Cukali Dome; CrD = Cretan Detachment; EMG = East Mainland Greece Detachment; EV = Elbasan-Vlora Transfer Zone; IA = Itea-Amphissa Detachment; JA = Jastrebac core complex; KB = Kosovo-Metohia Basin; KO = Kopaonik core complex; MH = Meso-Hellenic Basin; OD = Othoni-Dhermi Transfer Fault; PW = Peshkopie Window; SA = Sarajevo Basin; SV = Sava Suture Zone; SPNF = Shkoder-Peja Normal Fault.

Jurassic-Cretaceous pelagic sequence overlain by Paleogene flysch (Meço & Aliaj, 2000). The SPNF probably roots in incompetent Oligocene flysch at the top of the underlying Kruja Nappe, which is also an important detachment horizon for thrusting in the area southeast of the SPNF.

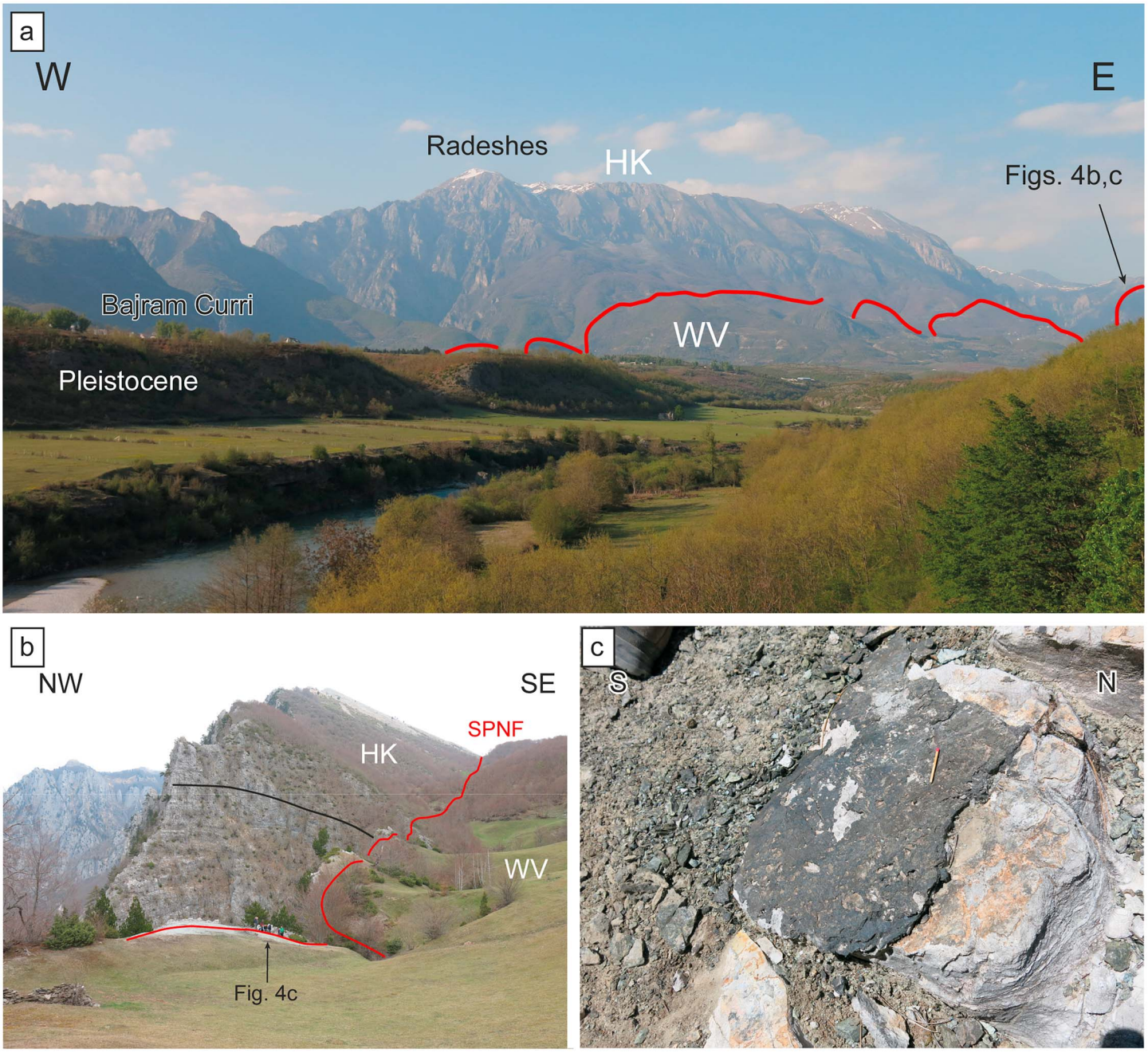

Figure 4. (a) Topographic relief associated with the Shkoder-Peja Normal Fault (SPNF) at the northern margin of the Tropoja Basin (location in Figure 5). Here the SPNF (red line) juxtaposes mélange of the West Vardar ophiolite unit (WV, hanging wall) with carbonates and flysch of the High Karst nappe (HK, footwall). Note in foreground the Pleistocene gravel terraces and abandoned river channels that document episodic incision and surface uplift of the entire area; (b) SPNF (red line) juxtaposes upper Triassic dolomitic marble of HK (footwall) with Jurassic mélange of the WV (hanging wall). Note downward drag of bedding in footwall (black line) toward the SPNF fault surface. Arrow points to outcrop in (c). Outcrop coordinates: 42.444134°, 20.158945° (42°26′38.9″N, 20°09′32.2″E); (c) Cataclasite of SPNF-ophiolitic mélange with components of serpentinite from hanging wall overlies foliated upper Triassic dolomitic marble (white). Match for scale; outcrop coordinates: 42.444134°, 20.158945° (42°26′38.9″N, 20°09′32.2″E).

The throw of the SPNF decreases gradually along strike from NE to SW, from a maximum estimate of about 7 km near the town of Bajram Curri (Figure 5a) to zero at Shkoder, where the normal fault ends (Figure 5c). There, the base of the West Vardar ophiolite nappe, including the underlying Jurassic mélange, is thrust directly onto olistolith-bearing flysch of the Krasta-Cukali nappe. The lack of the High-Karst and Pre-Karst nappes along this contact is attributed not to their tectonic omission but to

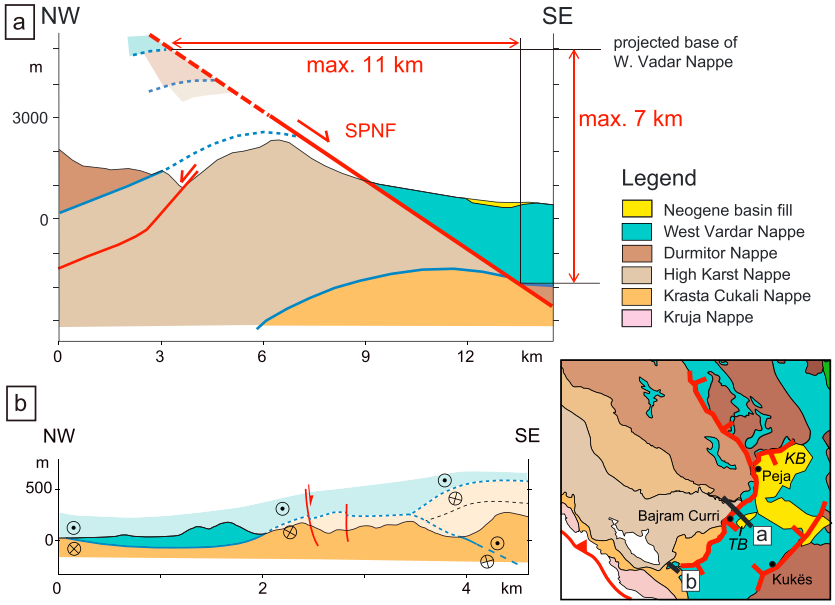

Figure 5. Cross sections showing NE-SW, along-strike decrease in vertical throw of the SPNF: (a) Baram Curri (Tropoja)—base of the West Vardar ophiolite nappe is offset vertically by some 7 km. Note Miocene Metohia Basin in the hanging wall and antiform exposing the High-Karst nappe in the footwall; (b) Shkoder—klippe of West Vardar ophiolite thrust directly onto Paleogene flysch of Krasta-Cukali Nappe; the Pre-Karst and High-Karst nappes are missing. The SPNF does not exist at this locality which is just west of the inferred clockwise rotation axis of the SPNF (text for explanation). Inset map modified from Schmid et al. (2008, 2011). TB = Tropoja Basin; KB = Kosovo-Metohia Basin; SPNF = Shkoder-Peja Normal Fault.

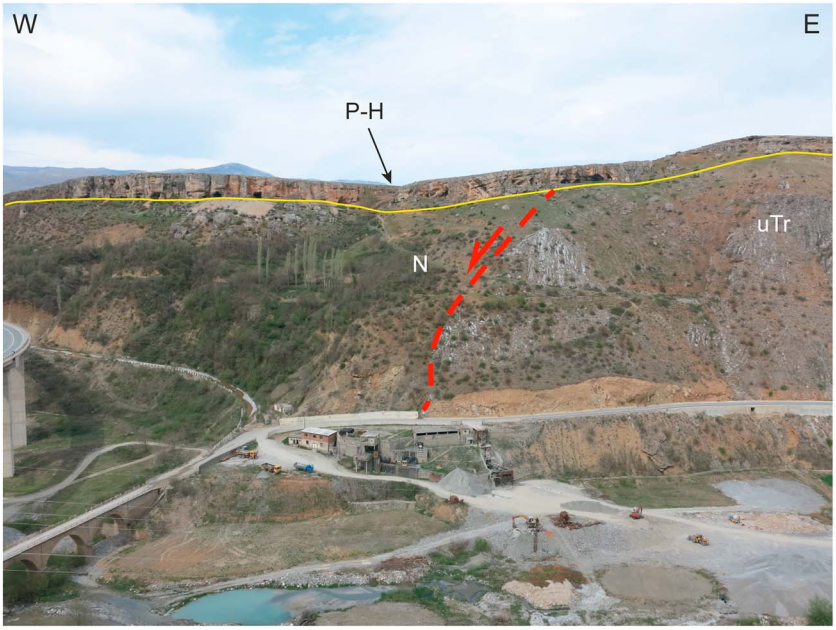

Figure 6. Miocene normal faulting at northern side of the entrance to the Luma Gorge near Kukes, NE Albania. Normal fault (red dashes with motion arrow of hanginwall) juxtaposes Upper Triassic limestone (uTr) of the Korab-Pelagonian Nappe in the footwall with Pliocene conglomerates (N) in the hanging wall. This faulted sequence is overlain by Pleistocene-Holocene terraces (P-H, above yellow line), which are in turn faulted and warped into a gentle monocline. Photo location coordinates: 42° 3′58.20″N, 20°27′54.39″E.

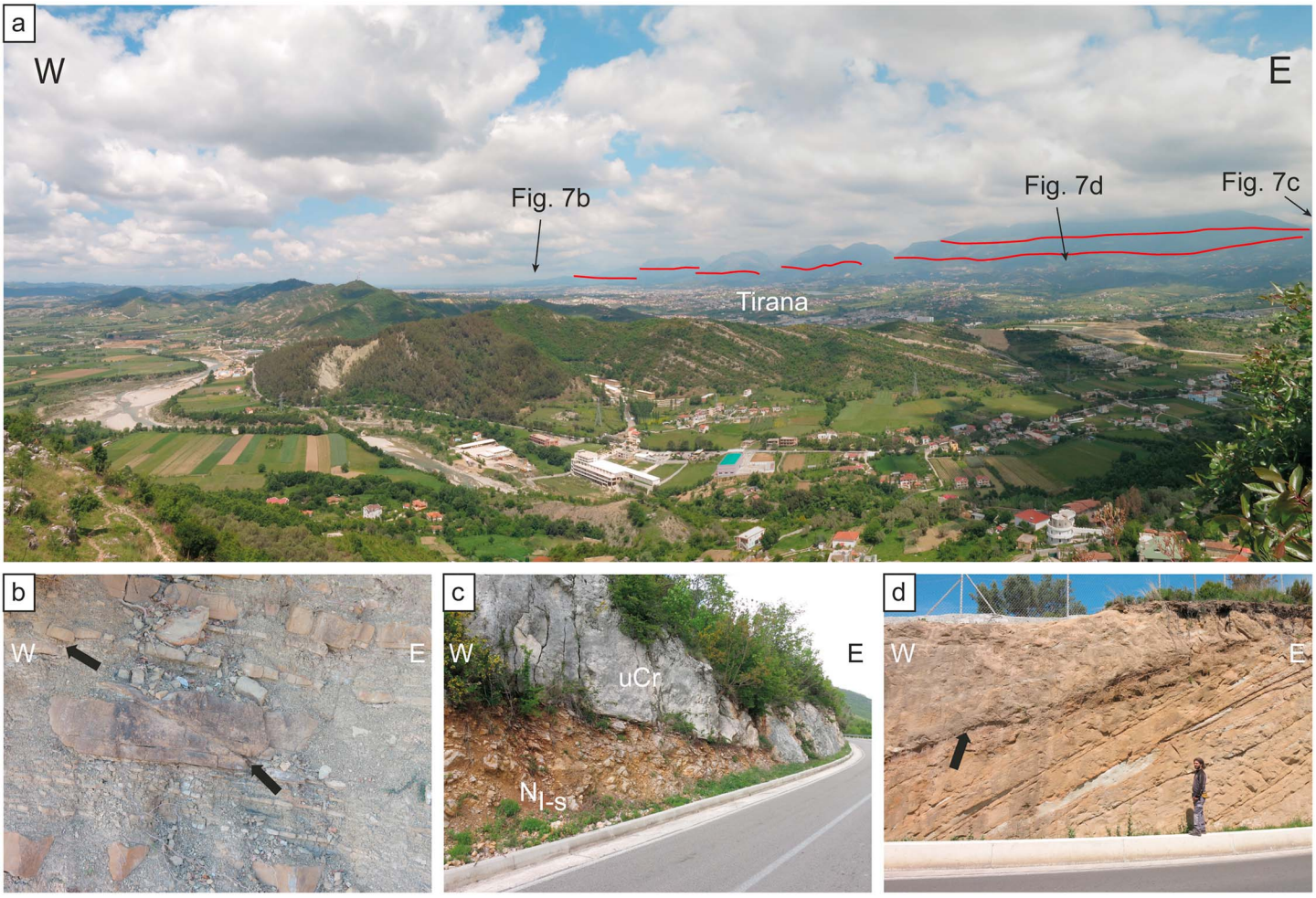

Figure 7. (a) Neogene thrust front (red line) along the Tirana Basin, Albania: Mountain range in background comprises imbricates of Mesozoic carbonates and Paleogene flysch of the Kruja Nappe thrust onto Neogene flysch. Note steepened bedding of backfolded and back-thrusted Neogene sediments in foreground. Coordinates: 41°15′23.37″N, 19°51′29.67″E; (b) faulted sandstone layers in Serravalian-Tortonian flysch (11.6 Ma) of the Kruja Nappe along the main thrust front on road above the town of Laci. Offset layers (arrows) indicate top-W thrusting. Coordinates: 41°37′54.04″N, 19°44′22.64″E; (c) thrust of upper Cretaceous limestone (uCr) onto brecciated Lithothamnian limestone ($N_{l\text{-}s}$, Langhian-Serravalian, 13.6 Ma) in the Kruja Nappe. Coordinates: 41°19′35.55″N, 19°56′40.93″E; (d) west-dipping bedding and unconformity (arrow) in Upper Miocene sandstone near town of Linze document progressive steepening during W-directed syn-sedimentary thrusting; older strata beneath the unconformity dip more steeply; coordinates: 37°25′19.1″N, 122°05′06″W.

earlier (pre-Neogene) dextral displacements controlled by the aforementioned along-strike Mesozoic facies change in which part of the Adriatic carbonate platform disappeared to the SE (Aubouin & Dercourt, 1975). The increase in throw of the SPNF from SW to NE between Shkoder and Bajram Curri indicates scissor-like extension of the crust in map view, with clockwise rotation of the hanging wall about a vertical rotation axis located at the SW end of the fault near Shkoder (red star in Figures 2 and 3). Given the average 30° dip of the SPNF in the Bajram Curri area (Figure 5a), we estimate a maximum horizontal displacement of some 11 km in the SE direction of extension in the western part of the Kosovo-Metohia Basin. Smaller horizontal displacements are possible given that the throw of 7 km is a maximum obtained by projecting the base of the West Vardar ophiolite nappe from along strike in the north into the plane of the section in Figure 5a.

The age of the SPNF is constrained by cross-cutting structures and Miocene syn-rift sediments. The SPNF offsets SW-vergent thrusts and folds of the Krasta-Cukali unit in its footwall, thus clearly postdating Eocene nappe transport in this part of the Dinarides and Hellenides. Orogen-parallel normal faulting initiated no later than the deposition of middle to late Miocene (16.4–7.1 Ma), syn-rift clastic sediments in the hanging wall of the SPNF (Elezaj, 2009; Elezaj & Kodra, 2012).

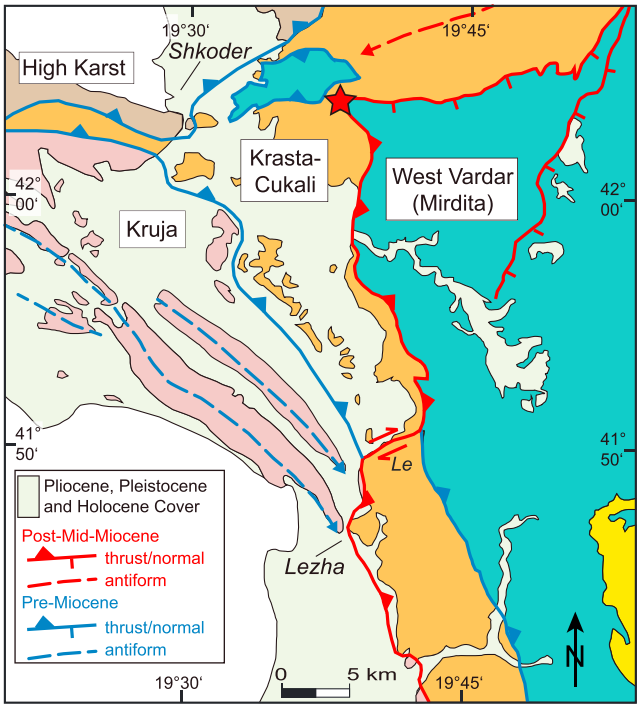

Figure 8. Tectonic map of the Lezha Transfer Fault (Le) along the Neogene thrust front, the Shkoder-Peja normal fault, and rotational axis (red star) based on own mapping and the Geological Map of Albania (Xhomo et al., 1999). Units and colors as in Figure 2.

The steep topographic gradient going from the Kosovo-Metohia Basin at 550 m above sea level to mountains in the footwall of the SPNF, some reaching up to 2,300 m above sea level (Figure 4a), strongly suggests very young to ongoing activity of the SPNF. Plio-Pleistocene deposits in the Kosova Basin comprise alluvial fans and fluvial terraces with abandoned river channels (Figure 4a).

A conjugate, NW-dipping normal fault SE of the SPNF near the town of Kukes (Figures 3 and 6) juxtaposes the top of the West Vardar ophiolite nappe and discordantly overlying Cretaceous carbonates in its hanging wall (the latter undifferentiated in the figures) with a structurally deeper, Adria-derived nappe (Korab-Pelagonian) in its footwall, amounting to a throw of some 1–2 km. This fault offsets late Miocene to Pliocene clastics and is sealed by late Pleistocene to Holocene layers, which are in turn deformed to a monocline (Figure 6).

Normal faults trending parallel to subparallel to the orogen, that is, at high angles to the SPNF, affect the nappe stack to the south and southeast of the Dinaride-Hellenide junction. They accommodate orogen-perpendicular displacement with throws of up to several kilometers, for example, along the western margin of the Peshkopie Window (Figure 3). There, Paleozoic basement and Mesozoic cover of the Adriatic distal margin (Korab-Pelagonian Nappe) in the footwall are juxtaposed with downthrown Jurassic clastics covering the Neotethyan West Vardar ophiolite in the hanging wall. This suggests a SW-dipping normal fault that excised almost the entire West Vardar ophiolite nappe. Another example is at the western boundary of the Neogene Burell Basin where an ENE-dipping normal fault juxtaposes West Vardar ophiolite in the footwall (Figure 3; Aliaj et al., 1995) with Neogene infill forming a broad synform in the hanging wall of this fault. Taken together, these observations indicate Mio-Pliocene extension normal to the strike of the orogen on both NE- and SW-dipping normal faults above asymmetrical rift basins (Figure 2).

Deformed Holocene beds (Figure 6) and extensional earthquake focal mechanisms (Pondrelli et al., 2006) indicate that orogen-parallel and orogen-normal extension is ongoing. In the Peshkopie Window, where normal faults trend parallel to the orogen, modeled apatite fission-track and fission-helium ages indicate that prolonged cooling beginning at ~20 Ma yielded to faster cooling from 6 to 4 Ma (Muceku et al., 2008).

3. Neogene Thrusting and Transfer Faulting

The mountain range forming the eastern morphological boundary of the Tirana Basin (internal subbasin of the Periadriatic Foredeep or Depression; Roure et al., 2004) is the site of Neogene thrusting and folding (Figure 7a, red lines). This is documented by deformed Tortonian clastic sediments with W-directed shear indicators (Figure 7b), as well as by W-directed thrusts of Mesozoic and Paleogene limestones onto Neogene foredeep sediments (Figure 7c). These thrusts offset Tortonian sediments deposited above the basal Seravallian unconformity that seals Paleogene thrusts and folds responsible for the older, main phase of shortening in the Kruja Nappe. These older structures were overprinted by Late Neogene shortening associated with open-to-tight folds, thrusts, and backthrusts affecting the Neogene deposits of the Tirana Basin (Gelati et al., 1997).

The Neogene thrust front in northern Albania is offset dextrally along two NE-SW-striking zones, here named the Lezha and Elbasan-Vlora Transfer Zones (Figures 8 and 9). Between the SPNF rotation axis at Shkoder and the Lezha Transfer Zone, the Neogene thrust runs within the flysch of the Krasta-Cukali Nappe and carries thin imbricates detached from the overlying Korab and the thick pile of West Vardar ophiolite units onto the Krasta-Cukali Nappe. At Lezha, the Paleogene folds of the structurally lower Kruja Nappe plunge beneath this thrust (Figure 8). From the Lezha Transfer Zone to the SE and all the way along the morphological front of the mountain belt to Tirana (Figure 7a), the Neogene thrusts imbricate Mesozoic-Paleogene strata of the Kruja Nappe (Figure 10a). Advance of the thrust front toward the foreland

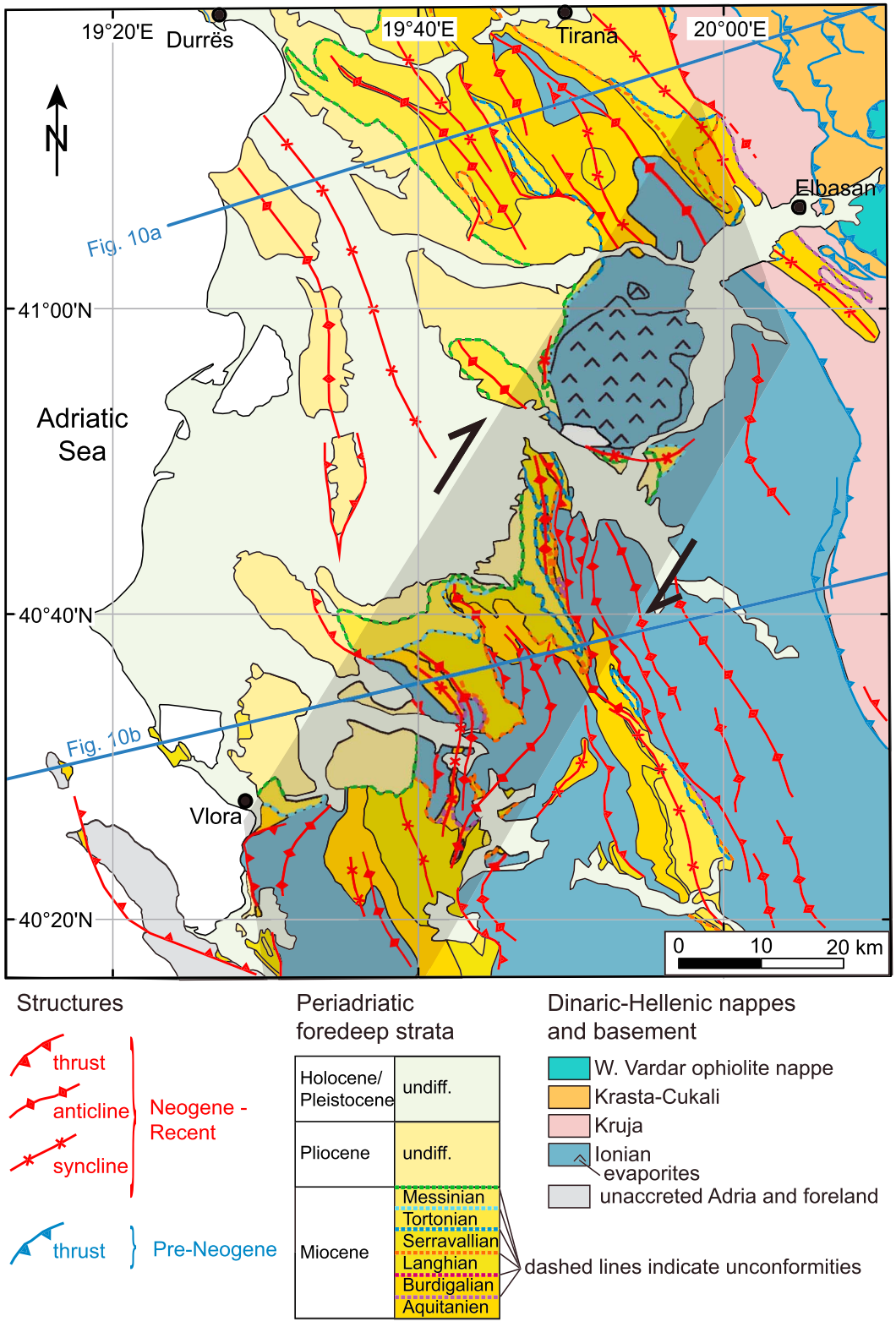

Figure 9. Tectonic map of the Elbasan-Vlora Transfer Zone (gray shaded area) dextrally offsetting the Neogene thrust front. Map based on 1:200,000 Geological Map of Albania (Xhomo et al., 1999) and own observations. Blue lines indicate traces of cross sections in Figure 10.

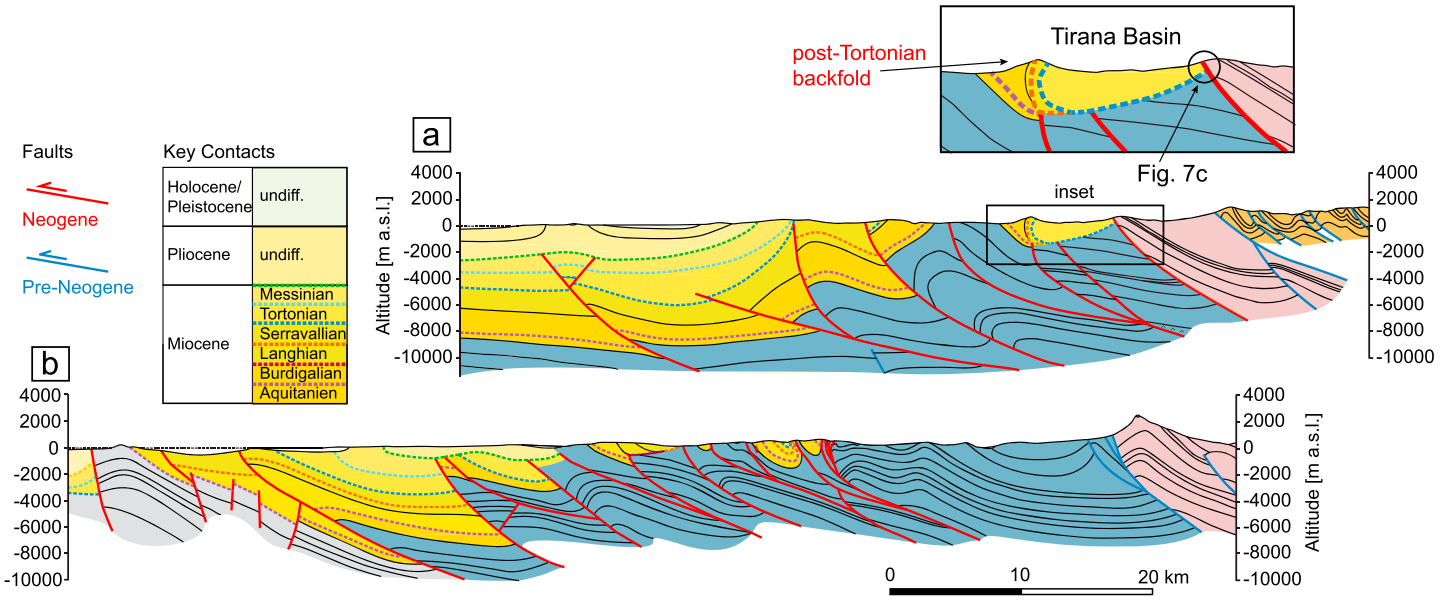

Figure 10. Cross sections across the Neogene thrust front north (a) and south (b) of the Elbasan-Vlora Transfer Zone shown in Figure 9. Cross sections modified from Xhomo et al. (2002).

during Late Neogene sedimentation is documented by W-dipping, onlap wedges in lower Miocene sediments (Figure 7d; Gelati et al., 1997). Between Tirana and Elbasan, the late Neogene thrusts are transitional along strike to open folds as shortening is transferred progressively across strike into Miocene sediments of the Periadriatic Foredeep. This is manifested by steepened Miocene strata (Figure 7a), backfolds, and locally even overturned thrusts (Figure 10a, inset) that affect Miocene and even Pliocene basin fill (Xhomo et al., 2002, their cross section IV).

The Elbasan-Vlora Transfer Zone offsets the Kruja and Ionian Nappes dextrally and to the SW (Figure 9). In map view, this transfer zone is marked by dextrally dragged folds and thrusts (Figure 9) as well as thrusts that steepen and offset all Neogene basal unconformities (Burdigalian, Serravallian, Tortonian, and Messinian; Xhomo et al., 2002, their cross sections V–VIII). The youngest tilted unconformity (basal Pliocene) occurs at the SW end of the transfer zone near Vlora (Figure 9). Taken together, the deformed unconformities indicate that the Elbasan-Vlora Transfer Zone has been active since at least middle Miocene time. A salt diapir in the middle of the zone (Figures 3 and 9) comprises Permo-Triassic salt from the decollement horizon of the Ionian thrust sheets. Miocene transfer faulting evidently exerted a control on the locus of diapirism (Bega & Soto, 2017), though final emplacement of the diapir is recent, as indicated by tilted Pleistocene beds in the outer limb of its rim syncline (Xhomo et al., 2002, their cross sections VI and VII).

The amount of post-mid-Miocene shortening south of the SPNF is inferred to increase southeastward with increasing distance from the SPNF rotation axis based on the NW-to-SE increase in topographic relief of the Neogene front toward Tirana (Figure 7a). This coincides with a dramatic orogen-parallel increase in the altitude of Tortonian clastics in the footwalls of thrusts, from a few tens of meters above sea level near Lezha (Figure 8) to >1,000 m in the structurally highest thrust sheets of the Kruja Nappe near Tirana (Figures 9 and 10a). Note, however, that between the SPNF rotation pole at Shkoder and the Elbasan-Vlora Transfer Zone, this Neogene shortening affects units above the SPNF detachment in the flysch of the Kruja Nappe. As argued below, this shortening is far less than that accommodated in the footwall of the Kruja Nappe.

A total of about 120 km of Neogene shortening is proposed for a published cross section across the orogenic front in the vicinity of the Elbasan-Vlora Transfer Zone (Bega & Soto, 2017; their section just north of our Figure 10b). This is corroborated by the across-strike distance of 100 km between correlative salt-bearing lithologies of the Ionian Nappe along the Neogene thrust front and in the Peshkopie Window, which represents the minimum amount of shortening at this locality. Most, if not all, of this Neogene shortening

occurred between Burdigalian and recent time (post-20.4 Ma) as indicated by thrusted and tilted unconformities in the Periadriatic Foredeep (Gelati et al., 1997; Xhomo et al., 1999, 2002).

The dextral displacement along the Elbasan-Vlora Transfer Zone is estimated to be about 28 km judging from map-view drag and offset of the basal thrust of the Kruja Nappe as well as of the thrust carrying the Krasta-Cukali Nappe and overlying West Vardar ophiolites onto the Kruja Nappe (Figure 9). As shown above, the post-Serravallian part of this total of 120 km shortening, which amounts to some tens of kilometers shortening within the Kruja Nappe and the Periadriatic Foredeep, is Tortonian and younger (<11.6 Ma). This constrains dextral motion of the Elbasan-Vlora Transfer Zone also to be of Tortonian and younger age.

In summary, most of the 100–120 km of Neogene shortening between the SPNF and the Elbasan-Vlora Transfer Zone occurred since Burdigalian time (20.4 Ma) and was accommodated above a detachment at the base of the Kruja Nappe. The hanging wall of this basal thrust includes the SPNF and its related Neogene thrusts which reactivate and imbricate Paleogene thrusts within the Kruja Nappe. This is a key point to which we return when determining the age and amount of crustal block rotation on the SPNF related to rollback subduction.

4. Oroclinal Bending of the Dinarides-Hellenides

4.1. Location, Age, and Rate of Bending

Paleomagnetic declination directions compiled in Figure 11 (references in the caption) indicate that the Dinarides-Hellenides junction has accommodated significant differential rotation. This is closely tied to the along-strike variations in Neogene shortening described above.

Declinations from Cretaceous and Eocene sediments in the southern Dinarides NW of the city of Dubrovnik are the same within error, indicating that there was no rotation of that part of the chain during this time span. However, declinations from Eocene sediments SE of Dubrovnik point more easterly than those in the NW, with the amount of rotation increasing to the SE across the Dinarides-Hellenides junction (Figure 11a). Where sampled, Oligocene sediments have the same declinations as the Eocene. The variation in declinations of Miocene sediments is even more striking, with northerly declinations at two localities in the Dinarides contrasting both with the more westerly Eocene declinations in the same area and with the progressively more easterly Miocene declinations south of the SPNF and across the Dinarides-Hellenides junction (Figure 11a). In units south of the SPNF in Figure 11a, Miocene declinations point more northerly than older declinations. In the Periadriatic Foredeep and the vicinity of the Elbasan-Vlora Transfer Zone (Figure 11b), the declinations with respect to Africa point ~N40°, with Miocene and Pliocene sediments showing slightly smaller angles.

Taken together, these data indicate that the length of orogen south of Dubrovnik in Figure 11a has undergone ~50° of clockwise arcuation relative to north since late Eocene-Oligocene time. Moreover, since the beginning of the Neogene, the Hellenic part of the orogen south of the SPNF has rotated clockwise by ~20° with respect to the Dinarides (and Europe; de Leeuw et al., 2012) and ~40° clockwise with respect to Africa (Figure 11b; Speranza et al., 1995; van Hinsbergen et al., 2005). A plot of declinations versus time using the same data for this area (Figure 11c) shows how the rate of this rotation has accelerated since Miocene time, with ~25° occurring in the past 5 Ma.

4.2. Relating Rotation to Along-Strike Variations in Dinarides-Hellenides Shortening

At first glance, it is tempting to relate the aforementioned NW-to-SE along-strike increase in Neogene shortening and rotation to the ~80-km dextral offset of the West Vardar ophiolite front that marks the SPTZ in map view (Figure 2). In such a scenario, the SPTZ acted like a clutch to accommodate differential Neogene shortening in the Dinarides and Hellenides. However, this interpretation can be ruled out on geological grounds because the dextral offset ends not at the Neogene orogenic front but in the Late Cretaceous-Paleogene Krasta-Cukali Nappe. The more external Kruja Nappe with its early-middle Oligocene flysch cover is not affected by this offset. The opposite, NE end of this offset, is within the internal Dinarides (Figure 2), where thrusting was no younger than Eocene (e.g., Schmid et al., 2008, and references therein). It follows from this that the dextral offset of the West Vardar ophiolite front across the SPTZ is a pre-Neogene

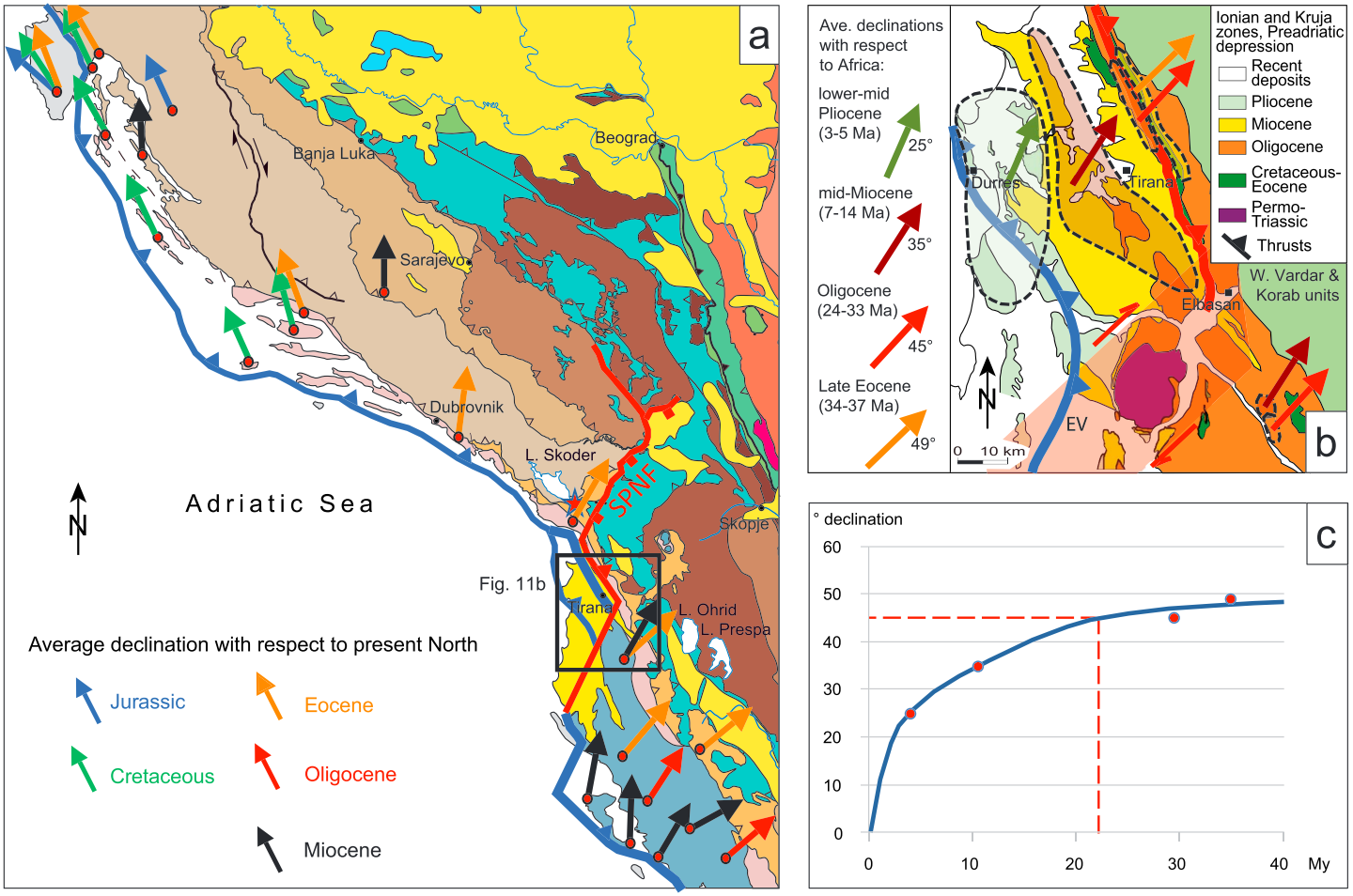

Figure 11. Paleomagnetic declinations in the Dinarides and northwestern Hellenides since time specified: (a) average declination with respect to present N as compiled from Marton et al. (2003, 2014) and de Leeuw et al. (2012 and references therein); blue line represents basal thrust system along orogenic front; red line represents SPNF system; EV = Elbasan-Vlora Transfer Zone; box outlines location of map in (b); (b) average declinations with respect to Africa from data of Speranza et al. (1995); map modified from their Figure 2) and van Hinsbergen et al. (2005); dashed lines outline sites analyzed for each age group; (c) plot of average declination versus age for data in (b); map units and faults in (a) from Schmid et al. (2011) and colored as in Figures 2 and 12, respectively. SPNF = Shkoder-Peja Normal Fault.

feature and cannot have accommodated differential Neogene shortening or rotation; it is overprinted by and therefore pre-dates the SPNF.

Instead, we attribute the southward increase in Neogene shortening along the Dinarides-Hellenides orogen to thrusting associated with clockwise oroclinal bending, as documented in Figure 11 and summarized above. Of the total ~50° of clockwise bending, ~40° rotation south of Dubvronik was broadly coeval with Neogene thrusting along the orogenic front and somewhat later in mid-Miocene time, with the beginning of extensional rotation on the SPNF. The Pliocene acceleration of rotation of the Hellenides south of the SPNF (Figure 11c) coincides with the ages of the youngest unconformities affected by thrusting and transfer faulting in the Periadriatic Foredeep (Figure 10). We therefore attribute the 25° bend of the Kruja nappe and its Paleogene folds near Shkoder (Figures 3 and 8) to Mio-Pliocene oroclinal bending. Morphological features in these folds (abandoned dry river beds and windgaps) have been interpreted as evidence of post-middle Miocene-to-recent uplift in the hanging wall of a main detachment at the seismogenic base of the Kruja Nappe (Biermanns et al., 2018).

The along-strike change in the amount of Neogene thrusting appears to be gradual across the Dinarides-Hellenides junction, with possible jumps in displacement restricted to the aforementioned Lezha and Elbasan-Vlora Transfer Zones. The Neogene front of the Kruja (Dalmatian) Nappe can be followed

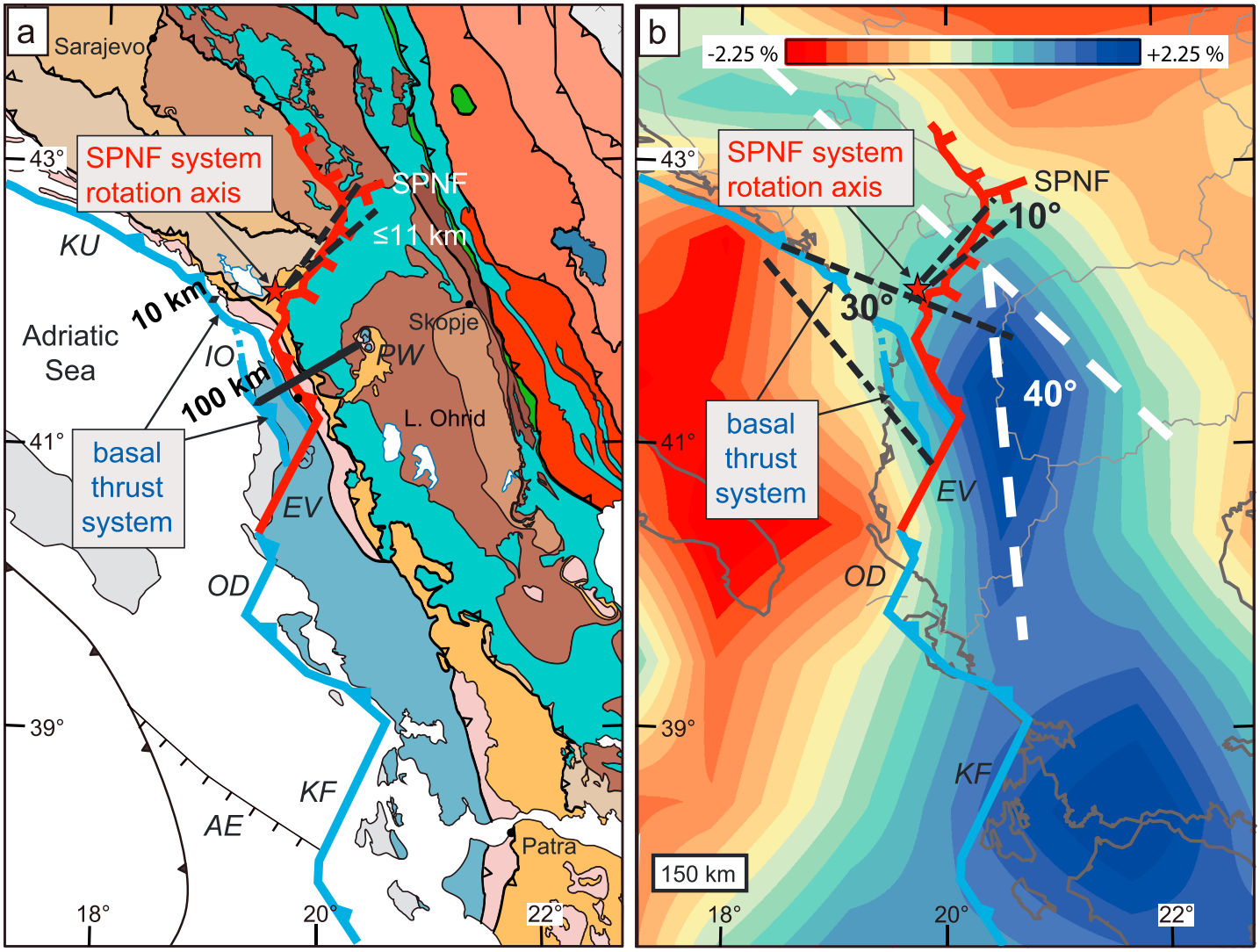

Figure 12. Constraints on Neogene shortening, extension, and rotation at the Dinarides-Hellenides junction: (a) displacements along the Kruja and Ionian thrust fronts (blue) NW and SE of SPNF; arrow shows 100-km minimum thrust distance between units of the Ionian Nappe exposed along the orogenic front and in the PW. Neogene thrust displacements of 10 km or less along the base of the Kruja Nappe NW of the SPNF from Bega (2015); (b) clockwise rotation angles associated with SPNF system (red) and basal thrust system (blue) superposed on *P* wave tomographic map of slab anomaly at 150-km depth (model UU-PO7 of Hall & Spakman, 2015); numbers represents displacements in kilometers (see text). EV = Elbasan-Vlora Transfer Zone; IO = Ionian nappe front; KF = Kefalonia Transfer Zone; KU = Kruja nappe front; OD = Othoni-Dhermi Transfer Zone; PW = Peshkopie Window; SPNF = Shkoder-Peja Normal Fault; red star represents clockwise rotation axis of SPNF system.

northwestward as minor thrusts and folds with <5–10 km displacement of Miocene strata in sections of offshore Croatia (Fantoni & Franciosi, 2009, their Figure 6) and Montenegro (Bega, 2015, his "Dalmation thrust front"; Unen et al., 2018, their Figure 3). Irregularities in the orogenic foredeep, basement topography, and subthrust Mesozoic platform morphology imaged in marine seismic surveys (Bega, 2013; Galatovic, 2007) are probably related to segmentation during knick-like bending of the orogen (Bega, 2015).

4.3. Constraints on Extension, Block Rotation, and thrusting related to the SPNF

Extension along the SPNF beginning at around 15 Ma about a vertical axis at Shkoder (Figure 8) necessitates clockwise rotation of units in the hanging wall of the SPNF above its basal decollement which, as shown above, is located in the top of the Kruja Nappe of the Paleogene Dinaric-Hellenic nappe stack. The angle of rotation obviously depends on the coherence of the hanging wall units, as well as the amount of horizontal extension along the SPNF, which we estimated above to be ≤11 km in a NW-SE direction in the Bajram

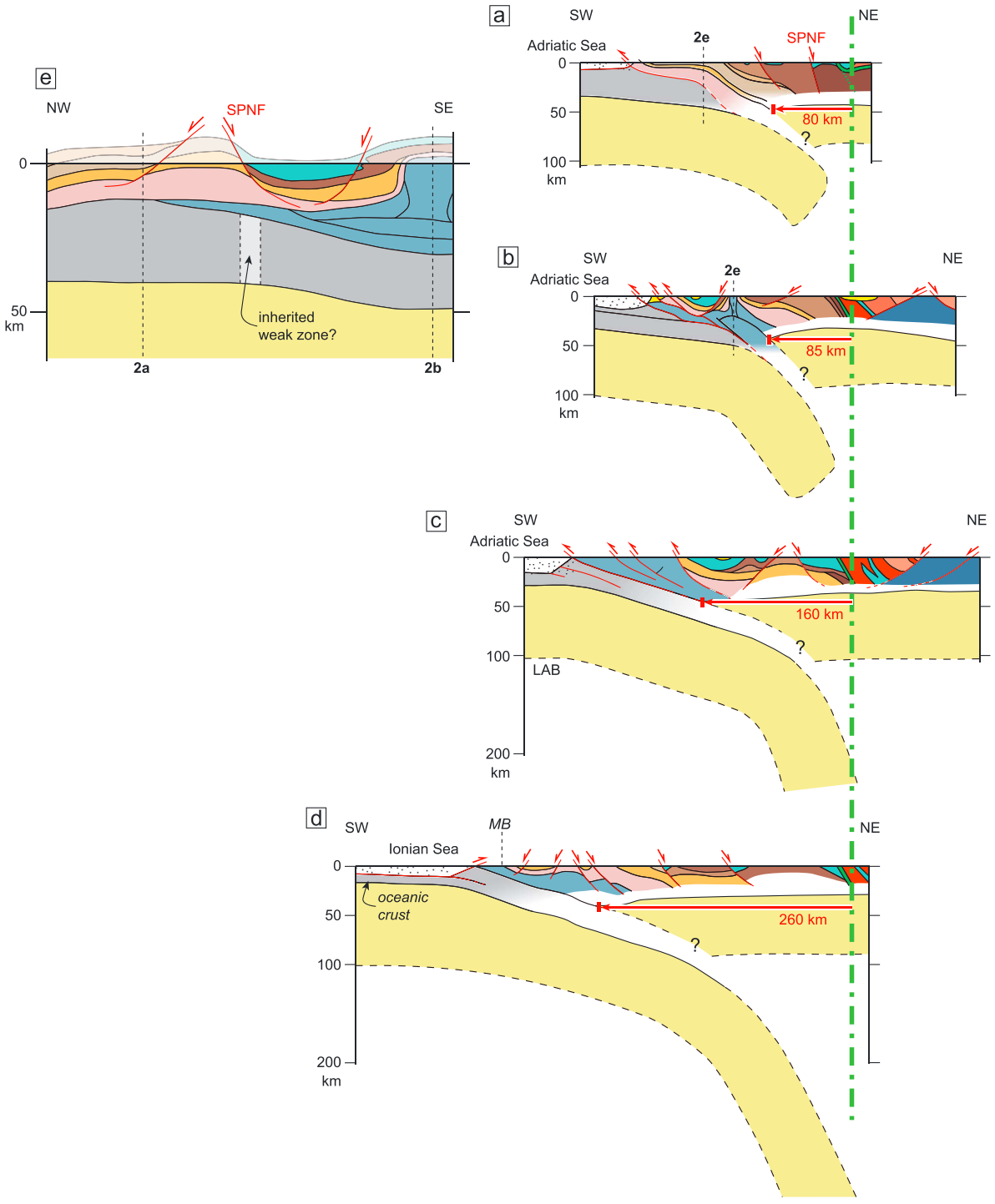

Figure 13. Cross sections orogen-perpendicular (a–d) to the Dinarides-Hellenides belt and orogen-parallel (e) across the Shkoder-Peja Normal Fault (SPNF); swath traces shown in Figures 1b and 2. Red lines show Neogene faults. Solid lines indicate well-constrained surfaces, and dashed lines are speculative surfaces. Geology simplified from compilations of Schmid et al. (2008, 2011) and cross sections of Bega (2015) and Bega and Soto (2017) for (a); Schenker et al. (2014), their Figure 1b) and Royden and Papanikolaou (2011), their Figure 7) for (c); Le Pichon et al. (2002), van Hinsbergen et al. (2005), their Figure 1b), and Jolivet et al. (2004), their Figure 3b) for (d), as well as the state geological maps of Albania (Xhomo et al., 1999) and Bornovas et al., 1983, and ex-Jugoslavia (Antonijević, 1969). MB = Mediterranean backstop; solid lines represent seismologically constrained MOHO in (a), (b), and (e) compiled from Sachpazi et al. (2007), Grad et al. (2009), and Delipetrov et al. (2016) and in (c) and (d) from Finetti (2005) and Pearce et al. (2012). Dashed lines represent poorly constrained MOHO. Lithosphere-Asthenosphere Boundary (LAB) compiled from Artemieva et al. 2006 (lower plate) and Sodoudi et al. (2006; upper plate in (c) and (d)). LAB of the slabs approximated from teleseismic *P* wave tomography of R. Hall and Spakman (2015), model UU-P07) and by assuming an average lithospheric thickness of 100 km (see Figures S1 and S2).

Curri area, decreasing to zero near Skhoder (Figure 5a). Assuming rigid, coherent behavior of the hanging wall, we obtain a maximum clockwise rotation of ~10° about the axis at Shkoder. This is much less than the total of ~50° post-Eocene-Oligocene clockwise rotation of Adriatic units with respect to present north in paleomagnetic studies of the Kruja und Ionian Nappes (Figure 13a) and also less than the ~40° post-mid-Miocene clockwise rotation with respect to Africa in the Periadriatic Foredeep south and west of the SPNF rotational axis (Figure 11b; Speranza et al., 1995; Kissel et al., 1995). Furthermore, it is less than the 25° change in strike of the Kruja Nappe going from northwest to southeast of Shkoder (Figures 2 and 3).

Given the ~10° of post-middle Miocene clockwise rotation of the SPNF hanging wall, E-W shortening along the SPNF decollement (i.e., in a direction subparallel to the syn-to-post Tortonian shear-sense directions plotted in Figure 3) is predicted to vary from 0 at the SPNF rotation axis to about 14 km at the latitude of the Elbasan-Vlora Transfer Zone. This falls well short of the aforementioned 100-km minimum estimate of total shortening from the Neogene orogenic front to the Peshkopie Window (Figure 12a), most of which was accommodated at the base of the Kruja Nappe during Burdigalian to Pliocene time. We attribute this discrepancy to partitioning of the rotational component of strain into a basal thrust running along the orogenic front and a structurally higher, out-of-sequence thrust that is kinematically linked with the SPNF detachment, as depicted in Figure 12 and discussed in the next section.

5. Relating Oroclinal Bending to Subduction

5.1. Quantifying Rollback Subduction

To assess how shortening and subduction are related to oroclinal bending, we quantify the amount of slab rollback in lithosphere-scale cross sections along and across the Dinarides-Hellenides junction (Figure 13). Slab rollback occurs when the down-going plate sweeps backward through the asthenosphere, causing the hinge in the lower plate—and therefore also the trench—to retreat away from a reference point on the upper plate. In the absence of a mantle reference frame that can also be related to the crust in this area, a useful proxy for rollback is the distance between the trace of the late Cretaceous Sava Suture Zone (Figure 2) projected to Moho depth and the present plate interface. This interface is taken to be the edge of the upper-plate Moho imaged in available Moho maps (Grad et al., 2009, for Figures 13a and 13b) and with high-resolution receiver functions and local earthquake tomography (Pearce et al., 2012; Halpaap et al., 2018, and references in caption for Figures 13c and 13d). We interpret the gap between the upper- and lower-plate Mohos in Figures 13a–13d to be filled with subducting crust that comprises external Dinaric-Hellenic and pre-Apulian units (Figure 2).

The Sava Suture Zone in Figures 13b–13d is assumed to extend steeply down to the Moho, although this is an oversimplification given that it probably flattens with depth due to lower crustal shearing during upper-plate extension. Tertiary stretching of the upper plate also affected the lithosphere NE of the Sava Suture Zone (e.g., Brun et al., 2016). Indeed, some workers argue that the same suture is exposed much further to the NE in the Rhodope unit of Figure 2 (Vardar Suture of Froitzheim et al., 2014; Brun et al., 2016). Thus, measuring the distance from the Sava Suture Zone at Moho depth to the current plate interface as proposed above yields only a minimum estimate of slab rollback since Adria-Europe suturing in latest Cretaceous time. Nevertheless, we argue below that rollback estimated in this way explains the observed clockwise oroclinal bending of the NW-Hellenides with respect to the southern Dinarides.

The slabs in Figure 13 are constrained at their upper ends by the lower-plate Moho inferred from seismological studies (references in figure captions) and by positive *P* wave anomalies from seismic tomography (model UU-P07 of Hall & Spakman, 2015; see Movie S1). The lower ends are poorly constrained due to defocusing effects and blurring of these anomalies with depth (Foulger et al., 2013). This renders depictions of slab length and inclination in Figure 13 only approximate, especially in the Dinarides where broadband seismic stations are few and the resolution is correspondingly poor.

5.2. Estimates of Plate-Interface Retreat

North of the SPNF (Figure 13a), the Adriatic slab anomaly is imaged to a depth of only ~160 km. A slab depth of <200 km beneath the southern Dinarides is also a feature of other global and Mediterranean-scale tomography studies involving independent imaging techniques and data sets (Bijwaard & Spakman, 2000; Koulakov et al., 2009; Piromallo & Morelli, 2003; Serretti & Morelli, 2011; Spakman & Wortel, 2004; Zhu

et al., 2012). In a local study using a relatively small data set and analyzed with an approximate local imaging method, Šumanovac et al. (2017) propose a much deeper slab anomaly reaching down to 400–450 km below most of the Dinarides. It is unclear from their work how well-resolved the imaged slab anomaly is because of the anomaly-smearing artifacts exposed in their checkerboard test (their Figure 6, particularly the vertical cross sections) and because of the limitations of this particular checkerboard test to assess spatial resolution (Rawlinson & Spakman, 2016). We therefore opt for a short slab (<200 km) in this transect as imaged in the global model UU-P07 used here (see Movie S2 for video of depth-dependent spatial resolution). As argued below, a short slab in Figure 13a is consistent with independent geological evidence for late Paleogene slab detachment in the Dinarides.

Using the approach outlined above, we obtain ~80 km of plate-interface retreat north of the SPNF (Figure 13a). The slab image in the cross section just south of the SPNF is longer, but the plate interface has retreated almost the same amount, 85 km (Figure 13b). Yet further to the south in the section across the Peloponnesus (Figure 13c), the slab image extends down to 240 km, and the amount of retreat increases to ~160 km. South of the Kefalonia Transfer Zone, where the slab penetrates the Mantle Transition Zone (Piromallo & Morelli, 2003, their Figure 9f) and Ionian oceanic lithosphere has entered the subduction zone, measured retreat attains some 260 km (Figure 13d). The orogenic crust and lithospheric mantle thicken slightly going from the Dinarides to the Hellenides across the SPNF (Figure 13e).

6. Discussion

The coincidence of anomalous fault kinematics at the Dinarides-Hellenides junction with along-strike changes in the geometry of the retreating Adriatic slab raises questions regarding the timing of slab rollback, the degree of crust-mantle coupling during rollback, and its effect on differential motion between the two subplates of Adria, the Hellenides, Africa, and Europe. Answering these questions sheds light on how motion of the mantle is transferred through the crust to the surface during rollback subduction, a central theme of this paper outlined in section 1.

6.1. How Does Bending of the Orogenic Crust Compare With Slab Geometry?

In Figure 12b, we use the contrasting estimates of Neogene shortening NW and SE of the SPNF to constrain a clockwise oroclinal bending angle of ~30°, delimited by dashed lines connecting the minimum shortening estimates along the basal Dalmatian-Kruja thrust in offshore Montenegro (Bega, 2013) and in Albania (Figure 12a and above). Note that due to poor constraints on shortening in the Dinarides, we do not know where, if at all, Neogene shortening drops to zero north of the SPNF. However, the dashed lines converge to a northern end of Neogene bending of the Dinaric-Hellenic chain in the vicinity of Dubrovnik. Bending angles <30° are possible if Neogene shortening exists further north along the Dinaric chain or >30° if Neogene shortening significantly exceeds the minimum estimates at the latitudes of the Peshkopie Window (100 km) and Elbasan-Vlora Transfer Zone (120 km).

Oroclinal bending of ~30° derived from Neogene shortening is in general agreement with the paleomagnetically derived estimates of Neogene rotation in the footwall of the SPNF in Figure 11. After Tortonian time, this rotation was accompanied by clockwise rotation of ~10° of the hanging wall of the SPNF (Figure 12b). Its contribution to shortening was transferred to the orogenic front at the base of the Ionian Nappe by the Elbansan-Vlora transfer zone (Figure 12a). The total amount of bending is therefore ~40°, with an error of ~10° given the uncertainties in the amounts of Miocene shortening along the chain and extension on the SPNF (Figure 12b).

Teleseismic *P* wave tomography at 150-km depth in Figure 12b indicates that the Adriatic slab anomaly bends sharply clockwise by ~40° in the vicinity of the SPNF (see also Movies S1 and S2, with sequential *P* wave tomographic depth slices and resolution tests in the range 100–160 km). The bend in the anomaly mimics the change in strike of the orogen at that location, as well as matches the amount of Miocene-Pliocene rotation described above. The map trace of this bent slab segment parallels the overall surface trace of Neogene-to-recent faults between the SPNF and the Kefalonia Transfer Zone (Figure 12). Crust and mantle structures are therefore coincident, suggesting that the entire orogenic lithosphere including the Adriatic foreland underwent bending during Hellenic rollback subduction.

This coincidence strongly suggests that the orogenic crust and mantle at the Dinarides-Hellenides junction have been mechanically coupled since at least early Miocene time. The orogen together with the upper plate have rotated while undergoing extension and dextral shearing to maintain compatibility with clockwise bending and retreat of the subducting lower plate.

6.2. When and Where Did Slab Breakoff and Rollback Affect the Dinaride-Hellenide Chain?

Rollback subduction of the Adriatic slab in the Dinarides started in late Eocene-Oligocene time as marked by extensive magmatism in half-graben systems that young from NE to SW toward the Dinaric foreland (Andrić et al., 2018). Earlier extension and magmatism in the hinterland of the Dinarides (Serbo-Macedonian and Circum-Rhodope units in Figure 2) in Late Cretaceous time (von Quadt et al., 2005) was broadly coeval with closure of the Neotethyan Sava Ocean (Gallhofer et al., 2015) but cannot be unequivocally linked to a rollback mechanism of subduction (Andrić et al., 2018). A belt of 34- to 22-Ma calc-alkaline magmatites (e.g., Andrić et al., 2018; Schefer et al., 2011) affecting parts of the internal Dinarides and units NE of the Sava Suture Zone, including the Carpatho-Balkan and Rhodopes (Figure 1a), is interpreted to mark removal of the slab, either by delamination (Schefer et al., 2011) or breakoff. In the vicinity of the Sava Suture Zone, shortening yielded to extension in late Oligocene time (Toljić et al., 2013; Erak et al., 2017; Stojadinović et al., 2017) when the orogenic front migrated SW into the external Dinarides (e.g., Unen et al., 2018). Extension involved the formation of latest Oligocene-Miocene metamorphic core complexes in the vicinity of the Sava Suture Zone (Bukulja, Kopaonik, Studenica, and Jastrebac core complexes in Figure 2) and early-to-middle Miocene extensional basins in the external Dinarides (Andrić et al., 2017). Extension was generally orogen-normal (E-W) and locally involved significant exhumation, for example, ~8 km in the footwall of the Busovača fault bounding the asymmetrical Sarajevo Basin (Figure 2; Unen et al., 2018). Following Matenco and Radivojević (2012), we attribute this early-mid-Miocene extension to the ~80-km retreat of the Adriatic slab beneath the Dinarides estimated in Figure 13a and/or to eastward pull of the extending Pannonian Basin to the east.

Extension and magmatism associated with rollback subduction in the southern Balkan peninsula (Andrić et al., 2018; Burchfiel et al., 2008) and Aegean region (Brun & Soukoutis, 2010; Royden & Papanikolaou, 2011) also began in Eocene-Oligocene time and swept from NE to SW, delaminating and thinning the upper plate of the retreating Hellenic arc-trench system (Brun et al., 2016; Jolivet & Brun, 2010). Recalling that our estimates of plate-interface retreat in Figures 13b–13d for the northern Hellenides are minima, we surmise that the amount of rollback across the Aegean toward the apex of the Hellenic arc was probably much greater (Jolivet & Brun, 2010; their Figure 9). As demonstrated in the previous sections, faster rollback and clockwise rotation of the Hellenides with respect to the Dinarides began in mid-Miocene time, corresponding to the main activity of the SPNF system. South and west of the SPNF, variously oriented normal faults and associated Miocene-Pliocene basins affect the northern Hellenides toward the present orogenic front in Albania and northern Greece (Burchfiel et al., 2008). Prominent Neogene extensional structures in the northern Hellenides include the Burell Basin and the Peshkopie Window (BU and PW in Figure 3), with the latter exposing Paleozoic basement that underwent rapid cooling in early Pliocene time (Muceku et al., 2008). Thus, a large area of upper-plate crust south of the SPNF was affected by both orogen-parallel and orogen-normal extension.

The contrasting amounts of plate-interface retreat and Neogene upper-plate extension north and south of the SPNF indicate that the Dinarides-Hellenides junction may have been the site of distributed dextral motion in addition to the rotational, orogen-parallel component of extension recorded by the SPNF system. The aforementioned metamorphic core complexes and Miocene basins in the internal Dinarides and Carpatho-Balkans define a narrow, late-Oligocene-Miocene extensional corridor that links the Carpathian-Pannonian Basin system to the north (Horváth et al., 2006) with the Hellenic-Aegean back-arc system to the south, as noted by Matenco and Radivojević (2012). The Kopaonik and Jastrebac core complexes within this corridor (Figure 3) have retrograde greenschist-facies mylonites with extensional directions varying from N-S to E-W, respectively (Erak et al., 2017; Mladenović et al., 2015; Schefer et al., 2011; Stojadinović et al., 2013, 2017). This large variation in local extension direction has been attributed to the close proximity of these core complexes to the Miocene rotation axis for opening of the Pannonian Basin behind the eastwardly expanding and retreating Carpathian orogen (Erak et al., 2017; Matenco & Radivojević, 2012).

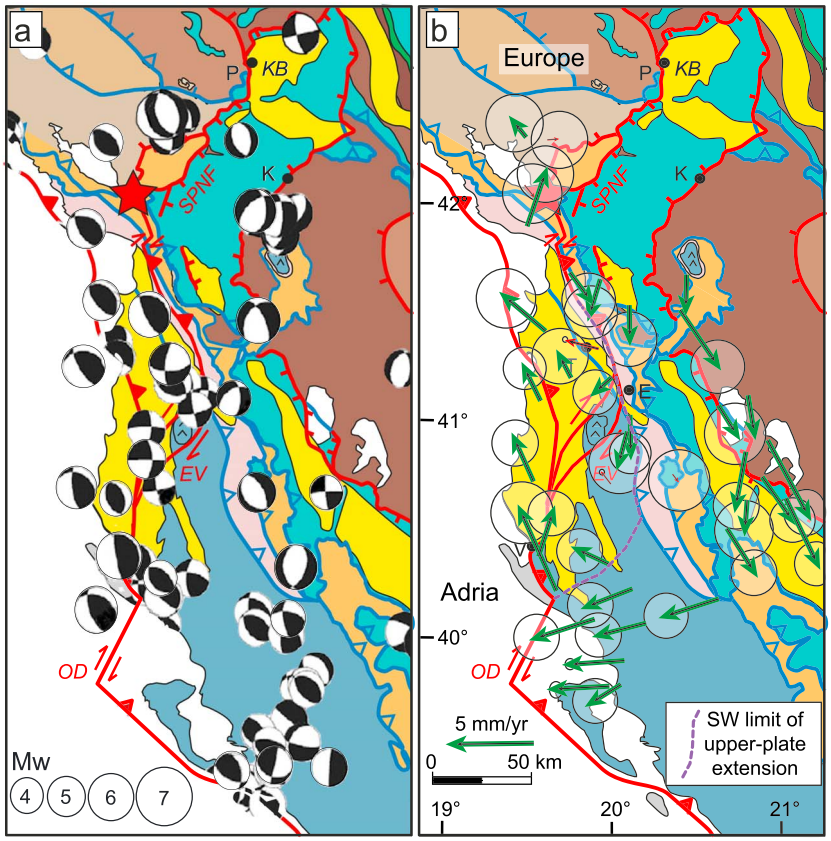

Figure 14. (a) Centroid Moment Tensor (CMT) catalogue focal mechanisms for Italy (1976–2012) and Europe (1997–2012) after Pondrelli et al. (2006); (b) GPS vectors with respect to Europe showing partitioning of shortening, extension, and block rotation due to rollback subduction in the Hellenides and NNW-directed Adria-Europe convergence, after Jouanne et al. (2012) and Métois et al. (2015). Tectonics units and abbreviations for localities as in Figures 2 and 3.

The Miocene pole of clockwise rotation for the retreating Hellenic arc and the Adriatic foreland is not the SPNF, as suggested in previous studies (e.g., Kissel et al., 1995; Walcott & White, 1998; van Hinsbergen et al., 2005) because we have shown that Miocene oroclinal bending and shortening affected the Dinaric-Hellenic chain and its foreland at least as far north as Dubrovnik (Figure 11). Therefore, we propose that the pole was located somewhere near Dubrovnik, possibly offshore of Dalmatia in Croatia (Figure 2). This is at the SE end of a submarine ridge, the Mid-Adriatic Ridge (Figure 1a), which is characterized by moderate seismicity on NW-SE striking thrusts and strike-slip faults (Scisciani & Calamita, 2009) that do not reach the mainland. Following D'Agostino et al. (2008), we propose that the MAR currently accommodates clockwise rotation of the Apulian subplate, which comprises Ionian oceanic lithosphere and continental lithosphere presently subducting beneath the Hellenic arc (Figure 1a).

Differences in tectonics across the Dinarides-Hellenides junction persist today, as revealed by the greater abundance of deep-level seismicity south of the SPNF (Pondrelli et al., 2006). Focal mechanisms at this junction indicate that the major Miocene structures, including the SPNF, have the same kinematics today as documented above in our structural studies (Figure 14a). Geodetic work indicates distributed shortening in the Dinarides (Bennett et al., 2008; Grenerczy et al., 2005), while in the Hellenides, shortening in external units of the chain contrasts with extension in internal units (Figure 14b; e.g., Hollenstein et al., 2008; Jouanne et al., 2012). The boundary between ongoing shortening and extension (dashed purple line in Figure 14b) runs SSE-ward from the SPNF rotational pole along the trace of Neogene out-of-sequence thrusts within the Kruja Nappe and then turns SW-ward to the orogenic front, skirting the southern border of the Elbasan-Vlora Transfer Zone. This transfer zone juxtaposes NW motion of Apulia to the north with gradual SW motion of the extending upper plate of the retreating Hellenic orogen with respect to Europe.

In summary, the current tectonic regime at the Dinarides-Hellenides junction appears to have been established already in early Miocene time when rollback subduction accelerated in the Hellenides (Brun et al., 2016). This drove clockwise rotation as well as deformation of the orogen and its foreland and possibly initiated the fragmentation the Adriatic Plate into its two current subplates, Adria s.str. and Apulia.

6.3. What Drove Bending and Rotational Extension at the Dinarides-Hellenides Junction?

To answer this question, we first discuss how slab anomalies in Figures 13a–13d reflect changes in the length of slab along Dinarides-Hellenides chain. The short slab image beneath the southern Dinarides in Figure 13a is interpreted to be a relic of an originally longer slab because shortening in the Dinaric thrust-and-fold belt, though not yet quantified, probably exceeded the current slab length of only ~160 km. Moreover, active-seismic studies cited in the previous section indicate that Neogene shortening in the Dinarides north of the SPNF amounted to no more than a few tens of kilometers (Bega, 2015). This contrasts with the longer slab images and greater Neogene shortening values obtained for the cross sections located south of the SPNF (Figures 13b–13d). Thus, the current slab length north of the SPNF (Figure 13a) is attributed primarily to Paleogene subduction, with only a minor contribution, if any, from Miocene-and-younger subduction. We propose that most of the Adriatic slab north of the SPNF was removed once Dinaric nappe stacking slowed or stopped in the late Eocene but during or just before the onset of Miocene upper-plate extension in the Dinarides. This leaves latest Eocene to Oligocene time as the probable range of time for slab removal, when widespread calc-alkaline magmatism affected parts of the internal Dinarides and units NE of the Sava Suture Zone (Figure 1a; Schefer et al., 2011; Andrić et al., 2018).

The amount of slab removed is a matter of conjecture; thermomechanical subduction models indicate that slabs beneath orogenic crust must be at least 200 km long for their downward pull force to overcome resistive forces and enable rollback (e.g., Chertova et al., 2014; Duretz et al., 2014; Hall et al., 2003). Applied to our case, these models suggest that rollback of the current slab beneath the Dinarides slowed and stopped after breakoff in Eocene-Oligocene time. We speculate that slab breakoff initiated with the southeastward propagation of a subhorizontal tear beneath the Dinarides (Wortel & Spakman, 2000) which then propagated obliquely downward to the SE along the slab in the vicinity of the Dinarides-Hellenides junction (Figure 15). Downward tearing may have been favored by a pre-existing weak zone at this junction, for example, related to the aforementioned Mesozoic transverse zone of Aubouin and Dercourt (1975) or the pre-Neogene SPTZ (above), as depicted schematically in Figures 13e and 15. This left the slab segment to the south beneath the Hellenides largely intact. Though speculative in the absence of high-resolution seismology, this scenario would account for the aforementioned lengthening of the slab anomaly along strike from the Dinarides to the Hellenides (Figure 13).

Slab tearing beneath the Dinarides is expected to have had a dramatic effect on the remaining part of the Adriatic slab to the south, with most action focused at the Dinarides-Hellenides junction as shown in Figure 15. The reduced slab mass above the putative tear in the Dinarides would have increased downward pull on the longer part of slab remaining beneath the Hellenides (bottom diagram in Figure 15b) in analogy with modeling studies of partial slab tearing (e.g., Duretz et al., 2014). Partial tearing in turn induced faster rollback to the SW and clockwise bending of the remaining slab along its torn edge in the vicinity of the Dinarides-Hellenides junction. Bending of the slab during slab retreat may have been enhanced by toroidal flow of asthenosphere around the slab edge (Funiciello et al., 2006). Though the main trigger of accelerated Hellenic rollback and Aegean extension appears to have been late Paleogene slab tearing in the Dinarides, it may have been augmented by rapid westward escape of Anatolia from mid-Miocene time onward (Brun et al., 2016).

Thus, pronounced orogen-parallel and orogen-normal extension of the Hellenic part of the chain south of the SPNF in mid-Miocene-Pliocene time was a direct response of the orogenic crust to bending of the Adriatic slab during accelerated rollback. Deformation of the upper plate to accommodate this slab motion was partitioned into a basal fold-and-thrust system affecting the Ionian and Kruja zones and into a structurally higher system of normal faults, most prominently the SPNF, that are linked to thrusts and transfer zones along the orogenic front (top diagram in Figure 15b). The rate of subduction in the southern Hellenides increased to its current value of 3.5 cm/year with the entrance of Mesozoic oceanic lithosphere of the Ionian Sea (Speranza et al., 2012) along the central part of the Hellenic trench in early-mid-Miocene time (Jolivet & Brun, 2010). By late middle Miocene time, about 15 Ma, Dinaric-Hellenic nappe

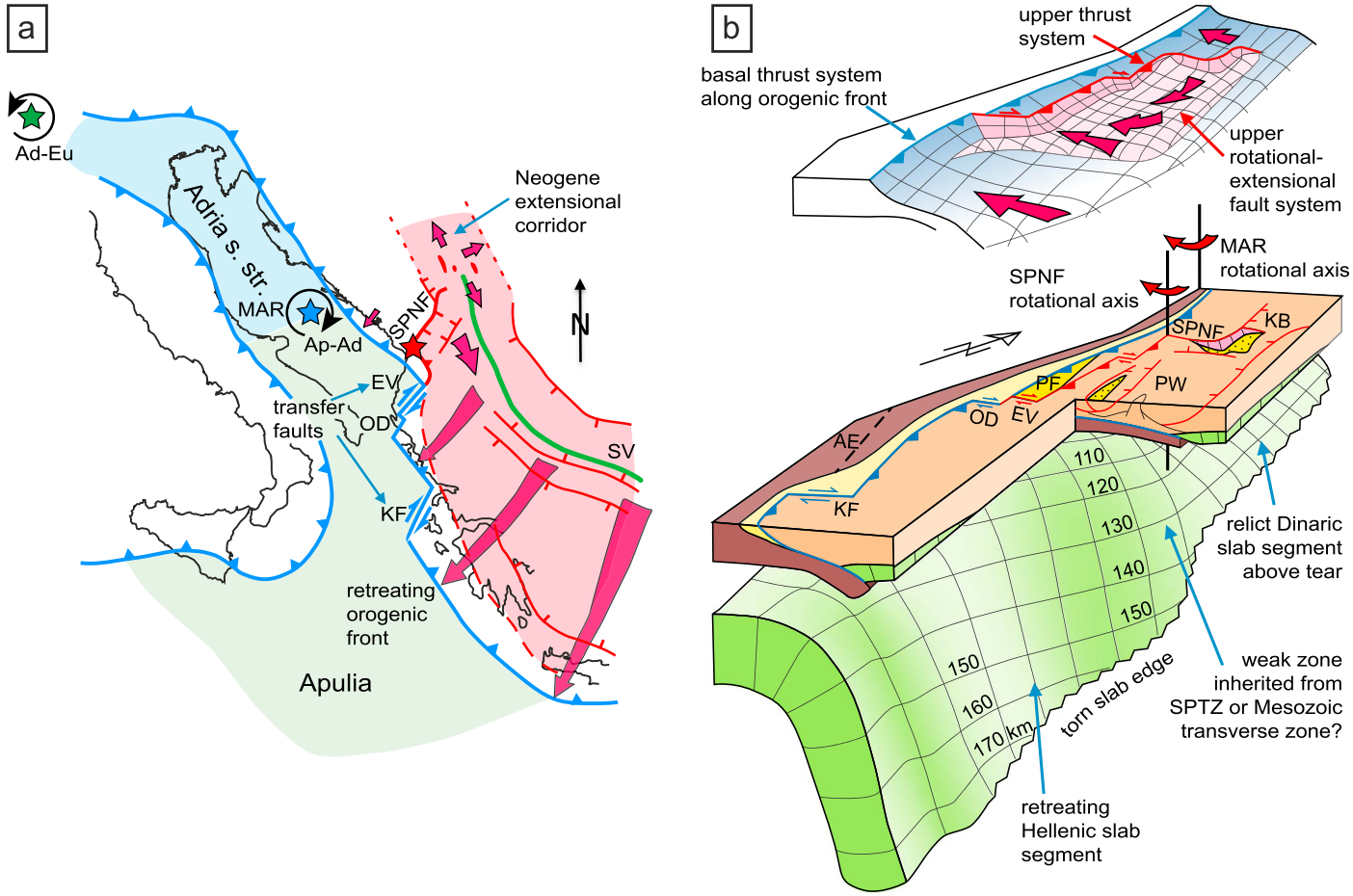

Figure 15. Model of the Neogene fault system at the Dinarides-Hellenides junction: (a) clockwise oroclinal bending and partitioning of vertical rotation into a basal thrust system along the orogenic front (blue) and an upper SPNF rotational system (red) that connects northward with a Neogene extensional corridor to the Pannonian Basin (red shaded); red spots mark metamorphic core complexes (see text); red star represents SPNF rotation axis; blue stars labeled Ad-Eu and Ad-Ap are the Neogene rotation axes, respectively, for Adria sensu stricto rotation relative to Europe and Apulia rotation relative to Adria sensu stricto and Europe (see text); (b, top diagram) topology of SPNF rotational extensional fault system (magenta, ≤15 Ma) linked by transfer faults and lateral ramps to the basal thrust system along the Dinaric-Hellenic orogenic front (blue). (bottom diagram) Neogene-to-Present plate boundary at the Dinarides-Hellenides junction with fault systems accommodating differential rollback of the Hellenic slab segment with respect to the torn Dinaric slab segment; red arrows represent Neogene-Present motion. AE = Adriatic Escarpment; EV = Elbasan-Vlora Transfer Zone; KB = Kosovo-Metohia Basin; KF = Kefalonia Transfer Zone; MAR = Mid-Adriatic Ridge; OD = Othoni-Dhermi Transfer Fault; PF = Periadriatic Foredeep; PW = Peshkopie Window; SPNF = Shkoder-Peja Normal Fault; SPTZ = Shkoder-Peja Transverse Zone; SV = Sava Suture Zone.

stacking had propagated rapidly SW to the present Mediterranean Backstop (Figure 2; Le Pichon et al., 2002) which forms the rigid buttress of a post-middle Miocene accretionary wedge fronting at the Mediterranean Ridge (Figure 1; Le Pichon et al., 2002). After 6–8 Ma, impingement of the Hellenic trench with the Mesozoic Adriatic Escarpment (Figures 2 and 15a) led to further segmentation of the orogenic front along the dextral Kefalonia Transfer Zone, where continental lithosphere continued to be subducted north of this fault (Royden & Papanikolaou, 2011). Subduction of the ocean-continent boundary south of the Kefalonia Transfer Zone gave rise to the present tectonic features of the Hellenic arc with abrupt, along-strike variations in subduction rate at zones of dextral transfer and arc-parallel extension.

6.4. Behavior of the Upper and Lower Plates

Neogene clockwise oroclinal bending and clockwise rotational extensional faulting on the SPNF at the Dinaride-Hellenide junction (Figure 12) coincided with NW-to-SE, along-strike increases in Neogene shortening (10 to 120 km), slab depth (160 to >280 km), and plate-interface retreat (80–260 km, Figure 13). This indicates that the crust and mantle in the upper and lower plates were coupled.

Fast shear-wave splitting (SKS) directions trend N-S to NE-SW beneath the upper plate in the northern Hellenides, indicating that prolonged flow of both the lithosphere (Endrun et al., 2011) and asthenosphere (Evangelidis, 2017) has occurred toward the retreating slab in the south. This inferred flow pattern is consistent with the overall direction of upper-plate extension associated with post-middle Miocene orogen-normal and orogen-parallel faulting on the SPNF and related faults, as well as with present extension directions indicated by earthquake focal mechanisms and GPS-derived motion vectors (Figure 14). Taken together, this suggests that the lithospheric flow pattern derived from the SKS directions has been established since mid-Miocene time. Uplifting and thinning of the upper plate above this inflowing mantle just behind the retreating slab is an attractive mechanism to explain the observed fluvial incision of Pleistocene terraces in the Kosovo-Metohia Basin (Figure 4a), although incision may have been enhanced by post-glacial rebound (Bathrellos et al., 2016).

Similar clockwise bending has been proposed for the Adriatic slab beneath the Kefalonia Transform Zone (Evangelidis, 2017; Halpaap et al., 2018) that dextrally offsets the Hellenic trench and the Mediterranean Backstop of offshore Peloponnesus (Figure 2; e.g., Louvari et al., 1999; Royden & Papanikolaou, 2011). However, in contrast with such slab bending, other parts of the slab away from the transform zone and beneath the Peloponnesus appear to be segmented into panels that step downward to the SE, that is, toward the apex of the Hellenic arc (Bocchini et al., 2018; Sachpazi et al., 2016). Where tears separating these panels have propagated up-dip to shallow depths, they are marked by zones of dextral offset or lateral ramping (Sachpazi et al., 2016). At the Dinarides-Hellenides junction, available seismological models are unable to resolve any tears in the lithosphere; the slab anomaly imaged in Figure 12b appears to bend rather than be broken into segments.

7. Conclusions

The junction of the Dinarides and Hellenides in northern Albania is marked by a Neogene-to-Recent fault system, most prominently the SPNF, that cuts a Late Cretaceous-Paleogene nappe stack formed during Adria-Europe collision (Figure 1). This fault system accommodated clockwise oroclinal bending and both orogen-parallel and orogen-normal extension in the upper plate of the SW-retreating Hellenic segment of the Adriatic slab. Across this fault system and along strike of the orogen, the Adriatic slab lengthens and bends, while the minimum amount of plate-interface retreat measured in cross sections increases from 80 to 260 km (Figure 13).

Deformation of orogenic crust at the Dinaride-Hellenide junction was partitioned into two structural levels: (1) a basal fold-and-thrust system in the Dalamatian-Kruja and Ionian Nappes that accommodated an increasing amount of SW-directed, Neogene shortening toward the apex of the Hellenic arc (Figure 12); and (2) a structurally higher system of faults, most notably the SPNF, affecting the Krasta-Cukali-Pindos Nappe and overlying nappes (Figures 3–6). Orogen-parallel, rotational extension along the SPNF and opening of the Kosovo-Metohia Basin in middle Miocene-to-Pliocene time were kinematically linked to out-of-sequence thrusting (Figure 7) and dextral transfer zones along the orogenic front in central and southern Albania (Figures 8–10). This fault system accommodated expansion of the rapidly retreating Hellenic subduction system that continues today (Figure 14). The orogen-parallel component of the SPNF differs from other upper-plate detachment systems with rotational axes in the Balkan-Aegean area that have accommodated orogen-normal extension of the upper plate since Eocene time (Figure 15a, references in caption).

Clockwise bending and arcuation of the Dinarides-Hellenides chain (Figures 11 and 12) is believed to have been triggered by late Paleogene tearing of the Adriatic slab beneath the Dinarides, which concentrated downward pull on the still-attached slab segment beneath the Hellenides. This enhanced rollback subduction of the Hellenides to the SW and bent the edge of this slab segment as far north as the SPNF (Figure 15b). The SPNF system transferred extension related to Hellenic rollback subduction northward into a narrow, orogen-parallel corridor that connected with broadly coeval Pannonian extension in the upper plate of the eastwardly retreating, Carpathian rollback system.

Rollback subduction has thus been the dominant process shaping the southern Dinarides and northern Hellenides, as well as their forelands since early Miocene time. The coincidence of the bend of the Adriatic slab beneath the Dinarides-Hellenides junction imaged by teleseismic *P* wave tomography with

the Mio-Pliocene fault kinematics described above (Figures 11, 12, and 14) suggests a high degree of coupling between the upper and lower plates at the NW end of the Hellenic subduction system.

Since early-mid Miocene time, the rotation pole for bending of the Dinaric-Hellenic orogen and indeed of the down-going plate has been located along the Mid-Adriatic Ridge in the Adriatic Sea, offshore, and well to the north of the SPNF (Figures 1a and 15b). This suggests that the Adriatic plate fragmented into two subplates (Adria s.str. and Apulia) and that the Apulian subplate, which is also attached to the Ionian Sea and Africa and is currently subducting beneath the Hellenic arc, has behaved nonrigidly. Future experiments invoking passive-array seismology may resolve the structures accommodating this behavior.

Acknowledgments
We thank Daniel Bernoulli, Bernhard Fügenschuh, Eline Le Breton, Douwe van Hinsbergen, Bruno Tomljenović, Liviu Matenco, and Marko Vrabec for discussions, as well as PhD and MSc students at the FU Berlin (S. Cionoiu, P. Groß, D. Goris, M. Grund, and S. Zertani) for mapping along the SPNF. Martina Grundmann and Marc Grund (FU-Berlin) helped draw figures for an earlier version of the manuscript. Jean-Pierre Brun provided a very constructive review, and Liviu Matenco and Gideon Rosenbaum made helpful suggestions on how to render the text more understandable. Grants of the German Science Foundation (DFG Projects Ha 2403/21-1, Gi 825/4-1, PI-534/3-1, and Us 100/5-1) and the Research Council of Norway, Centres of Excellence (project 223272) supported our research, and stipends of the German Academic Exchange Service (DAAD Promos fund, 2011–2017) partly funded student mapping and cooperation with colleagues in Albania. The data supporting this paper are available in the supporting information and references or by contacting the first author.

References

Aliaj, Sh., Melo, V., Hyseni, A., Skrami, J., Mehillka, L., Muco, B., et al. (1995). Neotectonic map of Albania. Tirana: Faculty of Energy and Mines, Republic of Albania

Anderson, H., & Jackson, J. (1987). Active tectonics of the Adriatic region. *Geophysical Journal of the Royal Astronomical Society*, *91*(3), 937–983. https://doi.org/10.1111/j.1365-246X.1987.tb01675.x

Andrić, N., Sant, K., Matenco, L., Mandic, O., Tomljenovi, B., Paveli, D., et al. (2017). The link between tectonics and sedimentation in asymmetric extensional basins: Inferences from the study of the Sarajevo-Zenica Basin. *Marine and Petroleum Geology*, *83*, 305–332. https://doi.org/10.1016/j.marpetgeo.2017.02.024

Andrić, N., Vogt, K., Matenco, L., Cvetković, V., Cloetingh, S., & Gerya, T. (2018). Variability of orogenic magmatism during Mediterranean-style continental collisions: A numerical modelling approach. *Gondwana Research*, *56*, 119–134. https://doi.org/10.1016/j.gr.2017.12.007

Antonijević, R. (1969). Geological Map of Jugoslavia. Belgrade: Federal Geological Survey.

Artemieva, I. M., Thybo, H., & Kaban, M. K. (2006). Deep Europe today: Geophysical synthesis of the upper mantle structure and lithospheric processes over 3.5 Ga. In D. Gee, & R. Stephenson (Eds.), *European Lithosphere Dynamics*, *Geological Society, London, Memoirs*, (Vol. 32, pp. 11–42).

Aubouin, J., & Dercourt, J. (1975). Les transversales dinariques dérivent-elles de paléofailles transformantes? *Comptes-Rendus Académie des Sciences, Série D*, *281*, 347–350.

Bathrellos, G. D., Skilodimou, H. D., & Maroukian, H. (2016). The significance of tectonism in the glaciations of Greece. In P. D. Hughes, & J. C. Woodward (Eds.), *Quaternary glaciation in the Mediterranean mountains*, *Geological Society,* London, Special Publications, (Vol. 433, pp. 237–250). http://doi.org/10.1144/SP433.5

Bega, Z. (2013). Deep seated platform carbonate reservoirs as new hydrocarbon plays in the NW Albania-Montenegro segment of the Adriatic region. Paper presented at the AAPG Conference, Barcelona, Spain, April 8-10, 2013.

Bega, Z. (2015). Hydrocarbon exploration potential of Montenegro. *Journal of Petroleum Geology*, *38*(3), 317–330. https://doi.org/10.1111/jpg.12613

Bega, Z., & Soto, J. I. (2017). Ionian fold-and-thrust belt in Central and Southern Albania—A petroleum province with Triassic evaporites. In J. I. Soto, J. Flinch, & G. Tari (Eds.), *Permo-Triassic salt provinces of Europe, North Africa and the Atlantic margins—Tectonics and hydrocarbon potential* (Chapt. 24, (pp. 517–542). Amsterdam, the Netherlands: Elsevier Inc. https://doi.org/10.1016/B978-0-12-809417-4.00025-2

Bennett, R. A., Hreinsdóttir, S., Buble, G., Bašić, T., Bačić, Ž., Marjanović, M., et al. (2008). Eocene to present subduction of southern Adria mantle lithosphere beneath the Dinarides. *Geology*, *36*(1), 3–6. https://doi.org/10.1130/G24136A.1

Bennett, R. A., Serpelloni, E., Hreinsdóttir, S., Brandon, M. T., Buble, G., Basic, T., et al. (2012). Syn-convergent extension observed using the RETREAT GPS network, northern Apennines, Italy. *Journal of Geophysical Research*, *117*, B04408. https://doi.org/10.1029/2011JB008744

Bernoulli, D. (2001). Mesozoic-Tertiary carbonate platforms, slopes and basins of the external Apennines and Sicily. In G. B. Vai (Ed.), *Anatomy Of An Orogen—The Apennines And Adjacent Mediterranean Basin*, (pp. 307–326). Kluwer Academic Publishers.

Biermanns, P., Schmitz, B., Ustaszewski, K., & Reicherter, K. (2018). Tectonic geomorphology and Quaternary landscape development in the Albania-Montenegro border region: An inventory. *Geomorphology*, *326*, 116–131. https://doi.org/10.1016/j.geomorph.2018.09.014

Bijwaard, H., & Spakman, W. (2000). Non-linear global P-wave tomography by iterated linearized inversion. *Geophysical Journal International*, *141*(1), 71–82. https://doi.org/10.1046/j.1365-246X.2000.00053.x

Bocchini, G. M., Brüstle, A., Becker, D., Meier, T., van Keken, P. E., Ruscić, M., et al. (2018). Tearing, segmentation, and backstepping of subduction in the Aegean: New insights from seismicity. *Tectonophysics*, *734-735*, 96–118. https://doi.org/10.1016/j.tecto.2018.04.002

Bornovas, J., Rondogianni-Tsiambaou, Th, & Papavassilou, K. (1983). Geological Map of Greece, 1:500,000, second edition. Institute of Geology and Mineral Exploration.

Bortolotti, V., Chiari, M., Marroni, M., Pandolfi, L., Principi, G., & Saccani, E. (2013). Geodynamic evolution of ophiolites from Albania and Greece (Dinaric-Hellenic belt): One, two, or more oceanic basins? *International Journal of Earth Sciences*, *102*(3), 783–811. https://doi.org/10.1007/s00531-012-0835-7

Brun, J.-P., Faccenna, C., Gueydan, F., Sokoutis, D., Philippon, M., Kydonakis, K., & Gorini, C. (2016). The two-stage Aegean extension, from localized to distributed, a result of slab rollback acceleration. *Canadian journal of Earth Sciences*, *53*(11), 1142–1157. https://doi.org/10.1139/cjes-2015-0203

Brun, J.-P., & Soukoutis, D. (2010). 45 m.y. of Aegean crust and mantle flow driven by trench retreat. *Geology*, *38*(9), 815–818. https://doi.org/10.1130/G30950.1

Burchfiel, B. C., Nakov, R., Dumurdzanov, N., Papanikolaou, D., Tzankov, T., Serafimovski, T., et al. (2008). Evolution and dynamics of the Cenozoic tectonics of the South Balkan extensional system. *Geosphere*, *4*(6), 919–938. https://doi.org/10.1130/GES00169.1

Channell, J. E. T., D'Argenio, B., & Horváth, F. (1979). Adria, the African promontory, in Mesozoic Mediterranean palaeogeography. *Earth Science Reviews*, *15*(3), 213–292. https://doi.org/10.1016/0012-8252(79)90083-7

Chertova, M. V., Spakman, W., Geenen, T., van den Berg, A. P., & van Hinsbergen, D. J. J. (2014). Underpinning tectonic reconstructions of the western Mediterranean region with dynamic slab evolution from 3-D numerical modeling. *Journal of Geophysical Research: Solid Earth*, *119*, 5876–5902. https://doi.org/10.1002/2014JB011150

Cvijić, J. (1901). Die dinarisch-albanische Scharung. Sitzungsberichte der kaiserlichen Akademie der Wissenschaften. Mathematisch naturwissenschaftliche Klasse CX. *Band Abtheilung*, *1*, 437–478.

D'Agostino, N., Avallone, A., Cheloni, D., D'Anastasio, E., Mantenuto, S., & Selvaggi, G. (2008). Active tectonics of the Adriatic region from GPS and earthquake slip vectors. *Journal of Geophysical Research*, *113*, B12413. https://doi.org/10.1029/2008JB005860

de Leeuw, A., Mandić, O., Krijgsman, W., Kuiper, K., & Hrvatović, H. (2012). Paleomagnetic and geochronologic constraints on the geodynamic evolution of the Central Dinarides, 2012. *Tectonophysics*, *530*(2), 286–298. https://doi.org/10.1016/j.tecto.2012.01.004

Delipetrov, T., Blazev, K., Doneva, B., & Popovski, R. (2016). Map of the Moho discontinuity of the Republic of Macedonia. Third Congress of Geologists of Republic of Macedonia, pp. 493-496.

Duretz, T., Gerya, T. V., & Spakman, W. (2014). Slab detachment in laterally varying subduction zones: 3-D numerical modeling. *Geophysical Research Letters*, *41*, 1951–1956. https://doi.org/10.1002/2014GL059472

Elezaj, Z. (2009). Cenozoic Molasse Basins in Kosova and their geodynamic evolution: Muzeul Olteniei Craiova. *Oltenia. Studii şi Comunicări. Ştiinţele Naturii. Craiova*, *25*, 348–349.

Elezaj, Z., & Kodra, A. (2012). *Geology of Kosovo. Ministria e Zhvillimit Ekonomik* (p. 300). Priština: Shtypshkronja Printing Press.

Endrun, B., Lebedev, S., Meier, T., Tirel, C., & Friederich, W. (2011). Complex layered deformation within the Aegean crust and mantle revealed by seismic anisotropy. *Nature Geoscience*, *4*(3), 203–207. https://doi.org/10.1038/NGEO1065

Erak, D., Matenco, L., Toljić, M., Stojadinović, U., Andriessen, P., Willingshofer, E., & Ducea, M. N. (2017). From nappe stacking to extensional detachments at the contact between the Carpathians and Dinarides—The Jastrebac Mountains of Central Serbia. *Tectonophysics*, *710*, 162–183.

Evangelidis, C. P. (2017). Seismic anisotropy in the Hellenic subduction zone: Effects of slab segmentation and subslab mantle flow. *Earth and Planetary Science Letters*, *480*, 97–106. https://doi.org/10.1016/j.epsl.2017.10.003

Faccenna, C., Jolivet, L., Piromallo, C., & Morelli, A. (2003). Subduction and the depth of convection in the Mediterranean mantle. *Journal of Geophysical Research*, *108*(B2), 2099. https://doi.org/10.1029/2001JB001690

Fantoni, R., & Franciosi, R. (2009). Tectono-sedimentary setting of the Po Plain and Adriatic Foreland. *Rendiconti Lincei*, *21*(Suppl 1), 197–209. https://doi.org/10.1007/s12210-010-0102-4

Finetti, I. R. (2005). *CROP Project: Deep Seismic Exploration of the Central Mediterranean and Italy. Atlases in Geoscience, 1, table 72*. Amsterdam: Elsevier.

Foulger, G. R., Panza, G. F., Artemieva, I. M., Bastow, I. D., Cammarano, F., Evans, J. R., et al. (2013). Caveats on tomographic images. *Terra Nova*, *25*(4), 259–281. https://doi.org/10.1111/ter.12041

Froitzheim, N., Jahn-Awe, S., Frei, D., Wainwright, A. N., Maas, R., Georgiev, N., et al. (2014). Age and composition of meta-ophiolite from the Rhodope Middle Allochthon (Satovcha, Bulgaria): A test for the maximum-allochthony hypothesis of the Hellenides. *Tectonics*, *33*, 1477–1500. https://doi.org/10.1002/2014TC003526

Funiciello, F., Moroni, M., Piromallo, C., Faccenna, C., Cenedese, A., & Bui, H. A. (2006). Mapping mantle flow during retreating subduction: Laboratory models analyzed by feature tracking. *Journal of Geophysical Research*, *111*, B03402. https://doi.org/10.1029/2005JB003792

Gallhofer, D., von Quadt, A., Peytcheva, I., Schmid, S. M., & Heinrich, C. A. (2015). Tectonic, magmatic and metallogenic evolution of the late Cretaceous arc in the Carpathian-Balkan Orogen. *Tectonics*, *34*, 1813–1836. https://doi.org/10.1002/2015TC003834

Gawlick, H.-J., Frisch, W., Hoxha, L., Dumitrica, P., Krystyn, L., Lein, R., et al. (2008). Mirdita Zone ophiolites and associated sediments in Albania reveal Neotethys Ocean origin. *International Journal of Earth Sciences*, *97*(4), 865–881. https://doi.org/10.1007/s00531-007-0193-z

Gawlick, H.-J., Missoni, S., Suzuki, H., Sudar, M., Lein, R., & Jovanović, D. (2016). Triassic radiolarite and carbonate components from a Jurassic ophiolitic mélange (Dinaridic Ophiolite Belt). *Swiss Journal of Geosciences*, *109*(3), 473–494. https://doi.org/10.1007/s00015-016-0232-5

Gelati, R., Diamanti, F., Prence, J., & Cane, H. (1997). The stratigraphic record of Neogene events in the Tirana Depression. *Rivista Italiana di Paleontologia e Stratigrafia*, *103*(1), 81–100.

Georgiev, N., Pleuger, J., Froitzheim, N., Sarov, S., Jahn-Awe, S., & Nagel, T. J. (2010). Separate Eocene–Early Oligocene and Miocene stages of extension and core complex formation in the Western Rhodopes, Mesta Basin, and Pirin Mountains (Bulgaria). *Tectonophysics*, *487*(1-4), 59–84. https://doi.org/10.1016/j.tecto.2010.03.009

Galatovic, B. (2007). Seismogenic model for Montenegro: Overview of relevant data. Paper presented at the first Workshop for the NATO Science for Peace Project, No. 983054, November 7-9, 2007, Slovenia.

Grad, M., Tiira, T., & ESC Working Group (2009). The Moho depth map of the European Plate. *Geophysical Journal International*, *176*(1), 279–292. https://doi.org/10.1111/j.1365-246X.2008.03919.x

Grenerczy, G., Sella, G., Stein, S., & Kenyeres, A. (2005). Tectonic implications of the GPS velocity field in the northern Adriatic region. *Geophysical Research Letters*, *32*, L16311. https://doi.org/10.1029/2005GL022947

Hall, C. E., Gurnis, M., Sdrolias, M., Lavier, L. L., & Müller, R. D. (2003). Catastrophic initiation of subduction following forced convergence across fracture zones. *Earth and Planetary Science Letters*, *212*(1-2), 15–30. https://doi.org/10.1016/S0012-821X(03)00242-5

Hall, R., & Spakman, W. (2015). Mantle structure and tectonic history of SE Asia. *Tectonophysics*, *658*, 14–45. https://doi.org/10.1016/j.tecto.2015.07.003

Halpaap, F., Rondenay, S., & Ottemüller, L. (2018). Seismicity, deformation, and metamorphism in the Western Hellenic Subduction Zone: New constraints from tomography. *Journal of Geophysical Research: Solid Earth*, *123*, 3000–3026. https://doi.org/10.1002/2017JB015154

Harangi, S., Downes, H., & Seghedi, J. (2006). Tertiary–Quaternary subduction processes and related magmatism in the Alpine Mediterranean region. *Geological Society, London, Memoirs*, *32*(1), 167–190. https://doi.org/10.1144/GSL.MEM.2006.032.01.10

Hollenstein, C., Müller, M. D., Geiger, A., & Kahle, H.-G. (2008). Crustal motion and deformation in Greece from a decade of GPS measurements, 1993–2003. *Tectonophysics*, *449*(1-4), 17–40. https://doi.org/10.1016/j.tecto.2007.12.006

Horváth, F., Bada, G., Szafian, P., Adam, M., & Cloetingh, S. (2006). Formation and deformation of the Pannonian Basin: constraints from observational data. In D. G. Gee & A. Stephenson (Eds)., European Lithosphere Dynamics, Geological Society, London, Memoirs (Vol. 32, pp. 191–206).

Jolivet, L., & Brun, J.-P. (2010). Cenozoic evolution of the Aegean. *International Journal of Earth Sciences*, *99*(1), 109–138. https://doi.org/10.1007/s00531-008-0366-4

Jolivet, L., Rimmelé, G., Oberhänsli, R., Goffé, B., & Candan, O. (2004). Correlation of syn-orogenic tectonic and metamorphic events in the Cyclades, the Lycian nappes and the Menderes massif. Geodynamic implications. *Bulletin de la Société Géologique de France*, *175*(3), 217–238. https://doi.org/10.2113/175.3.217

Jouanne, F., Mugnier, J. L., Koci, R., Bushati, S., Matev, K., Kuka, N., et al. (2012). GPS constraints on current tectonics of Albania. *Tectonophysics*, *554*, 50–62. https://doi.org/10.1016/j.tecto.2012.06.008

Kissel, C., Speranza, F., & Milicević, V. (1995). Paleomagnetism of external southern and central Dinarides and northern Albanides: Implications for the Cenozoic activity of the Scutari-Pec transverse zone. *Journal of Geophysical Research*, *100*(B8), 14999–15007. https://doi.org/10.1029/95JB01243

Koulakov, I., Kaban, M. K., Tesauro, M., & Cloetingh, S. (2009). P- and S velocity anomalies in the upper mantle beneath Europe from tomographic inversion of ISC data. *Geophysical Journal International*, *179*(1), 345–366. https://doi.org/10.1111/j.1365-246X.2009.04279.x

Le Breton, E., Handy, M. R., Molli, G., & Ustaszewski, K. (2017). Post-20 Ma motion of the Adriatic plate—New constraints from surrounding orogens and implications for crust-mantle decoupling. *Tectonics*, *36*, 3135–3154. https://doi.org/10.1002/2016TC004443

Le Pichon, X., Lallement, S. J., Chamot-Rooke, N., Lemeur, D., & Pascal, G. (2002). The Mediterranean Ridge backstop and the Hellenic nappes. *Marine Geology*, *186*(1-2), 111–125. https://doi.org/10.1016/S0025-3227(02)00175-5

Legler, C., Stanek, K.P., Dickmayer, E., Knoblock, A. (2006). Tectonic map of Kosovo, 1:200.000. Independent Commission for Mines and Minerals, Priština, Kosovo and Beak Consultants

Louvari, E., Kiratzi, A. A., & Papazachos, B. C. (1999). The Cephalonia Transform Fault and its extension to western Lefkada Island (Greece). *Tectonophysics*, *308*(1-2), 223–236. https://doi.org/10.1016/S0040-1951(99)00078-5

Marton, E., Ćosović, V., & Moro, A. (2014). New stepping stones, Dugi otok and Vis islands, in the systematic paleomagnetic study of the Adriatic region and their significance in evaluations of existing tectonic models. *Tectonophysics*, *611*, 141–154. https://doi.org/10.1016/j.tecto.2013.11.016

Marton, E., Drobne, K., Ćosović, V., & Moro, A. (2003). Palaeomagnetic evidence for Tertiary counterclockwise rotation of Adria. *Tectonophysics*, *377*(1-2), 143–156. https://doi.org/10.1016/j.tecto.2003.08.022

Matenco, L., & Radivojević, D. (2012). On the formation and evolution of the Pannonian Basin: Constraints derived from the orogenic collapse recorded at the junction between the Carpathians and Dinarides. *Tectonics*, *31*, TC6007. https://doi.org/10.1029/2012TC003206

Meço, S., & Aliaj, S. (2000). *Geology of Albania*. (246 pp). Berlin, Stuttgart: Gebruder Borntraeger.

Métois, M., D'Agostino, N., Avallone, A., Chamot-Rooke, N., Rabaute, A., Duni, L., et al. (2015). Insights on continental collisional processes from GPS data: Dynamics of the peri-Adriatic belts. *Journal of Geophysical Research: Solid Earth*, *120*, 8701–8719. https://doi.org/10.1002/2015JB012023

Mladenović, A., Trivić, B., & Cvetković, V. (2015). How tectonics controlled post-collisional magmatism within the Dinarides: Inferences based on study of tectono-magmatic events in the Kopaonik Mts. (Southern Serbia). *Tectonophysics*, *646*, 36–49. https://doi.org/10.1016/j.tecto.2015.02.001

Muceku, B., van der Beek, P., Bernet, M., Reiners, P., Mascle, G., & Tashko, A. (2008). Thermochronological evidence for Mio-Pliocene late orogenic extension in the north-eastern Albanides (Albania). *Terra Nova*, *20*(3), 180–187. https://doi.org/10.1111/j.1365-3121.2008.00803.x

Nocquet, J.-M., & Calais, E. (2004). Geodetic Measurements of Crustal Deformation in the Western Mediterranean and Europe. *Pure and Applied Geophysics*, *161*, 661–681. https://doi.org/10.1007/s00024-003-2468-z

Nopcsa, F. (1911). Zur Tektonik der Dinariden. *Zentralbl Mineral Geology Palaeontol*, *7*, 434–438.

Oldow, J., Ferranti, L., Lewis, D. S., Campbell, J. K., D'Argenio, B., Catalano, R., et al. (2002). Active fragmentation of Adria, the north African promontory, central Mediterranean orogen. *Geology*, *30*(9), 779–782. https://doi.org/10.1130/0091-7613(2002)030%3C0779:AFOATN%3E2.0.CO;2

Pamić, J. (2002). The Sava-Vardar Zone of the Dinarides and Hellenides versus the Vardar Ocean. *Eclogae Geologicae Helvetiae*, *95*, 99–113.

Pamić, J., Gusić, I., & Jelaska, V. (1998). Geodynamic evolution of the Central Dinarides. *Tectonophysics*, *297*(1-4), 251–268. https://doi.org/10.1016/S0040-1951(98)00171-1

Pearce, F. D., Rondenay, S., Sachpazi, M., Charalampakis, M., & Royden, L. H. (2012). Seismic investigation of the transition from continental to oceanic subduction along the western Hellenic Subduction Zone. *Journal of Geophysical Research*, *117*, B07306. https://doi.org/10.1029/2011JB009023

Pécskay, Z., Lexa, J., Szakács, X., Seghedi, I., Balogh, K., Konečný, V., et al. (2006). Geochronology of Neogene magmatism in the Carpathian arc and intra-Carpathian area. *Geologica Carpathica*, *57*(6), 511–530.

Piromallo, C., & Morelli, A. (2003). P wave tomography of the mantle under the Alpine-Mediterranean area. *Journal of Geophysical Research*, *108*(B2), 2065. https://doi.org/10.1029/2002JB001757

Pondrelli, S., Salimbeni, S., Ekström, G., Morelli, A., Gasperini, P., & Vannucci, G. (2006). The Italian CMT dataset from 1977 to the present. *Physics of The Earth and Planetary Interiors*, *159*(3-4), 286–303. https://doi.org/10.1016/j.pepi.2006.07.008, http://mednet.rm.ingv.it/quick_rcmt.php

Prelević, D., Wehrheim, S., Reutter, M., Romer, R. L., Boev, B., Bozović, M., et al. (2017). The Late Cretaceous Klepa basalts in Macedonia (FYROM)—Constraints on the final stage of Tethys closure in the Balkans. *Terra Nova*, *29*(3), 145–153. https://doi.org/10.1111/ter.12264

Rawlinson, N., & Spakman, W. (2016). On the use of sensitivity tests in seismic tomography. *Geophysical Journal International*, *205*(2), 1221–1243. https://doi.org/10.1093/gji/ggw084

Robertson, A. H. F., & Shallo, M. (2000). Mesozoic-Tertiary tectonic evolution of Albania in its regional Eastern Mediterranean context. *Tectonophysics*, *316*(3-4), 197–254. https://doi.org/10.1016/S0040-1951(99)00262-0

Roure, F., Nazaj, S., Mushka, K., Fili, I., Cadet, J.-P., & Bonneau, M. (2004). Kinematic evolution and petroleum systems—An appraisal of the Outer Albanides. In K. R. McClay (Ed.), *Thrust tectonics and hydrocarbon systems*, *AAPG Memoir*, (Vol. 82, pp. 474–493).

Royden, L. H., & Papanikolaou, D. J. (2011). Slab segmentation and late Cenozoic disruption of the Hellenic arc. *Geochemistry, Geophysics, Geosystems*, *12*, Q03010. https://doi.org/10.1029/2010GC003280 ISSN: 1525-2027

Sachpazi, M., Galvé, A., Laigle, M., Hirn, A., Sokos, E., Serpetsidaki, A., et al. (2007). Moho topography under central Greece and its compensation by Pn time-terms for the accurate location of hypocenters: The example of the Gulf of Corinth 1995 Aigion earthquake. *Tectonophysics*, *440*(1-4), 53–65. https://doi.org/10.1016/j.tecto.2007.01.009

Sachpazi, M., Laigle, M., Charalampakis, M., Diaz, J., Kissling, E., Gesret, A., et al. (2016). Segmented Hellenic slab rollback driving Aegean deformation and seismicity. *Geophysical Research Letters*, *43*, 651–658. https://doi.org/10.1002/2015GL066818

Sachpazi, M., Laigle, M., Charalampakis, M., Sakellariou, D., Flueh, E., Sokos, E., et al. (2016). Slab segmentation controls the interplate slip motion in the SW Hellenic subduction: New insight from the 2008 Mw6.8 Methoni interplate earthquake. *Geophysical Research Letters*, *43*, 9619–9626. https://doi.org/10.1002/2016GL070447

Sani, F., Vannucci, G., Boccaletti, M., Bonini, M., Corti, G., & Serpelloni, E. (2016). Insights into the fragmentation of the Adria Plate. *Journal of Geodynamics*, *102*, 121–138. https://doi.org/10.1016/j.jog.2016.09.004

Schefer, S., Cvetković, V., Fügenschuh, B., Kounov, A., Ovtcharova, M., Schaltegger, U., & Schmid, S. M. (2011). Cenozoic granitoids in the Dinarides of southern Serbia: Age of intrusion, isotope geochemistry, exhumation history and significance for the geodynamic evolution of the Balkan Peninsula. *International Journal of Earth Sciences*, *100*(5), 1181–1206. https://doi.org/10.1007/s00531-010-0599-x

Schenker, F.-L., Burg, J.-P., Kostopoulos, D., Moulas, E., Larionov, A., & von Quadt, A. (2014). From Mesoproterozoic magmatism to collisional Cretaceous anatexis: Tectonomagmatic history of the Pelagonian Zone, Greece. *Tectonics*, *33*, 1552–1576. https://doi.org/10.1002/2014TC003563

Schmid, S.M., Bernoulli, D., Fügenschuh, B., Matenco, L., Schefer, S., Oberhänsli, R., et al. (2011). First-order similarities and differences between the Alps, Dinarides, Hellenides and the Anatolides-Taurides. Paper and poster presented at the AGU Fall meeting, 2011, San Francisco, USA. See also https://tecto.earth.unibas.ch//images/ALCADI_2016_01_30.png

Schmid, S. M., Bernoulli, D., Fügenschuh, B., Matenco, L., Schuster, R., Schefer, S., et al. (2008). The Alpine-Carpathian-Dinaridic orogenic system: Correlation and evolution of tectonic units. *Swiss Journal of Geosciences*, *101*(1), 139–183. https://doi.org/10.1007/s00015-008-1247-3

Scisciani, V., & Calamita, F. (2009). Active intraplate deformation within Adria: Examples from the Adriatic region. *Tectonophysics*, *476*, 57–72. https://doi.org/10.1016/j.tecto.2008.10.030

Seghedi, L., & Downes, H. (2011). Geochemistry and tectonic development of Cenozoic magmatism in the Carpathian–Pannonian region. *Gondwana Research*, *20*(4), 655–672. https://doi.org/10.1016/j.gr.2011.06.009

Serretti, P., & Morelli, A. (2011). Seismic rays and traveltime tomography of strongly heterogeneous mantle structure: Application to the Central Mediterranean. *Geophysical Journal International*, *187*(1), 1708–1724. https://doi.org/10.1111/j.1365-246X.2011.05242.x

Sodoudi, F., Kind, R., Hatzfeld, D., Priestley, K., Hanka, W., Wylegalla, K., et al. (2006). Lithospheric structure of the Aegean obtained from P and S receiver functions. *Journal of Geophysical Research*, *111*, B12307. https://doi.org/10.1029/2005JB003932

Spakman, W., & Wortel, M. J. R. (2004). A tomographic view on Western Mediterranean geodynamics. Chapter 2. In W. Cavazza, F. M. Roure, G. M. Stampfli, & P. A. Ziegler (Eds.), *The Transmed Atlas—The Mediterranean region from crust to mantle*, (pp. 31–52). Berlin: Springer.

Speranza, F., Islami, I., Kissel, C., & Hyseni, A. (1995). Paleomagnetic evidence for Cenozoic clockwise rotation of the external Albanides. *Earth and Planetary Science Letters*, *129*(1-4), 121–134. https://doi.org/10.1016/0012-821X(94)00231-M

Speranza, F., Minelli, L., Pignatelli, A., & Chiappini, M. (2012). The Ionian sea: The oldest in situ ocean fragment of the world? *Journal of Geophysical Research*, *117*, B12101. https://doi.org/10.1029/2012JB009475

Stojadinović, U., Matenco, L., Andriessen, P., Toljić, M., Rundić, L., & Ducea, M. N. (2017). Structure and provenance of Late Cretaceous-Miocene sediments located near the NE Dinarides margin: Inferences from kinematics of orogenic building and subsequent extensional collapse. *Tectonophysics*, *710*, 184–204.

Stojadinović, U., Matenco, L., Andriessen, P. A. M., Toljić, M., & Foeken, J. P. T. (2013). The balance between orogenic building and subsequent extension during the Tertiary evolution of the NE Dinarides: Constraints from low-temperature thermochronology. *Global and Planetary Change*, *103*, 19–38. https://doi.org/10.1016/j.gloplacha.2012.08.004

Šumanovac, F., Markušić, S., Engelsfeld, T., Jurković, K., & Orešković, J. (2017). Shallow and deep lithosphere slabs beneath the Dinarides from teleseismic tomography as the result of the Adriatic lithosphere downwelling. *Tectonophysics*, *712*(2017), 523–541. https://doi.org/10.1016/j.tecto.2017.06.018

Toljić, M., Matenco, L.,Ducea, M. N., Stojadinović, U., Milivojević, J., & Đerić, N. (2013). he evolution of a key segment in the Europe-Adria collision: The Fruška Gora of northern Serbia. *Global and Planetary Change*, *103*, 39–62. https://doi.org/10.1016/j.gloplacha.2012.10.009

Tremblay, A., Meshi, A., Deschamps, T., Goulet, F., & Goulet, N. (2015). The Vardar zone as a suture for the Mirdita ophiolites, Albania: Constraints from the structural analysis of the Korabi-Pelagonia zone. *Tectonics*, *34*, 352–375. https://doi.org/10.1002/2014TC003807

Unen, M. V., Matenco, L., Nader, F. H., Darnault, R., Mandić, O., & Demir, V. (2018). Kinematics of foreland-vergent crustal accretion: Inferences from the Dinarides evolution. *Tectonics*, *38*, 49–76. https://doi.org/10.1029/2018TC005066

Ustaszewski, K., Kounov, A., Schmid, S. M., Schaltegger, U., Krenn, E., Frank, W., & Fügenschuh, B. (2010). Evolution of the Adria-Europe plate boundary in the northern Dinarides: From continent-continent collision to back-arc extension. *Tectonics*, *29*, TC6017. https://doi.org/10.1029/2010tc002668

Ustaszewski, K., Schmid, S. M., Fügenschuh, B., Tischler, M., Kissling, E., & Spakman, W. (2008). A map-view restoration of the Alpine-Carpathian-Dinaridic system for the Early Miocene. *Swiss Journal of Geosciences*, *101*(suppl. 1), 273–294. https://doi.org/10.1007/s00015-008-1288-7

van Hinsbergen, D. J. J., & Schmid, S. M. (2012). Map view restoration of Aegean–West Anatolian accretion and extension since the Eocene. *Tectonics*, *31*, TC5005. https://doi.org/10.1029/2012TC003132 issn: 0278-7407

van Hinsbergen, D. J. J., Zachariasse, W. J., Wortel, M. J. R., & Meulenkamp, J. E. (2005). Underthrusting and exhumation: A comparison between the External Hellenides and the "hot" Cycladic and "cold" South Aegean core complexes (Greece). *Tectonics*, *24*, TC2011. https://doi.org/10.1029/2004TC001692

van Hinsbergen, D. J. J., Mensink, M., Langereis, C. G., Maffione, M., Spalluto, L., Tropeano, M.,& Maffione, M. (2014). Did Adria toatet with respect to Africa? *Solid Earth*, *5*, 611–629. https://doi.org/10.5194/se-5-611-2014

von Quadt, A., Moritz, R., Peytcheva, I., & Heinrich, C. A. (2005). 3: Geochronology and geodynamics of Late Cretaceous magmatism and Cu–Au mineralization in the Panagyurishte region of the Apuseni–Banat–Timok–Srednogorie belt, Bulgaria. *Ore Geology Reviews*, *27*(1-4), 95–126. https://doi.org/10.1016/2005.07.024

Vrabec, M., Pavlovčić Prešeren, P., & Stopar, B. (2006). GPS study (1996-2002) of active deformation along the Periadriatic fault system in northeastern Slovenia-tectonic model. *Geologica Carpathica*, *57*(1), 57–65.

Walcott, C. R., & White, S. H. (1998). Constraints on the kinematics of postorogenic extension imposed by stretching lineations in the Aegean area. *Tectonophysics*, *298*(1-3), 155–175. https://doi.org/10.1016/S0040-1951(98)00182-6

Wortel, M. J. R., & Spakman, W. (2000). Subduction and slab detachment in the Mediterranean-Carpathian region. *Science*, *290*, 1910–1917. https://doi.org/10.1126/science.290.5498.1910

Xhomo, A., Nazaj, Sh., Nakuci, V., Yzeiraj, D., Lula, F., Sadushi, P., et al. (1999). Geological map of Albania (1:200.000). Tirana: Ministry of Industry and Energy, Ministry of Education and Science, Albanien Geological Survey, AlpPetrol, Polytechnical University of Tirana.

Xhomo, A., Nazaj, Sh., Nakuci, V., Yzeiraj, D., Lula, F., Sadushi, P., et al. (2002). Geological cross sections of Albania (1:200.000). Tirana: Ministry of Industry and Energy, Ministry of Education and Science, Albanien Geological Survey, AlpPetrol, Polytechnical University of Tirana.

Zhu, H., Bozdag, E., Peter, D., & Tromp, J. (2012). Structure of the European upper mantle revealed by adjoint tomography. *Nature Geoscience*, *5*(7), 493–498. https://doi.org/10.1038/NGEO1501